

(s, C<sub>6</sub>H<sub>4</sub>). <sup>13</sup>C NMR (ether): δ = 32.9 and 34.7 (2 CH<sub>3</sub>), 47.1 and 50.5 (C(1,3)), 115.9 (*p*-C), 121.8 (2 *o*-C), 122.7 and 123.1 (C(4,7)), 126.0 and 126.4 (C(5,6)), 127.9 (2 *m*-C), 149.2 (ipso-C), 152.3 and 154.6 (C(8,9)), 160.3 (C(2)), 184.1 (C<sub>α</sub>).

The colorless powder, as collected above, contained the "dimerization" product previously<sup>22</sup> isolated from the Grignard analogue of 5. It was detected under the present conditions even though we had earlier<sup>22</sup> reported that it was not observed by bromine/lithium exchange.

**Crystal Structure Determination.** The sample was sealed under argon in a glass capillary. Cell constants were determined by a least-squares fit of the setting angles of 25 centered reflections between 2θ = 18–25°. Lorentz and polarization corrections were applied in data collection (see Table IV).

**Structure Solution and Refinement.** It was difficult to obtain a good model by direct methods (SHELXS-86,<sup>24</sup> PC version), and a very high number (1200) of possible solutions had to be calculated in order to get starting positions for a model refining well with isotropic thermal parameters. This model showed the tetramethylindan fragments. The remaining non-hydrogen atoms

were found from a difference-Fourier map. The position of the Li atom emerged after assigning part of the carbon anisotropic thermal parameters. All hydrogen atoms were located and their positions refined with fixed  $U_i = 1.2U(\text{eq})$  from  $U(\text{eq})$  of the hydrogen-bearing carbon atoms. The structure was refined using the SHELXTL-PLUS<sup>25</sup> program package with full matrix least-squares procedures. The solution converged slowly but steadily.

**Acknowledgment.** Support by the Deutsche Forschungsgemeinschaft and the Fonds der Chemischen Industrie is gratefully acknowledged.

**Supplementary Material Available:** Tables of crystal data, fractional coordinates, bond distances, bond angles, anisotropic thermal parameters, and fractional coordinates of hydrogen atoms (12 pages). Ordering information is given on any current masthead page. Structure factor amplitudes are available on request from the author.

OM910770

(24) Sheldrick, G. M. SHELXS-86, Program for the automatic solution of crystal structures. University of Göttingen, Göttingen, Germany, 1986.

(25) Sheldrick, G. M. SHELXTL-PLUS, Version 4.1. Nicolet XRD, Madison, WI, 1987.

## Synthesis, Structure, Dynamic Behavior, and Reactivity of Chiral Rhenium Primary Phosphine and Phosphido Complexes of the Formula $[(\eta^5\text{-C}_5\text{H}_5)\text{Re}(\text{NO})(\text{PPh}_3)(\text{PRH}_2)]^+\text{X}^-$ and $(\eta^5\text{-C}_5\text{H}_5)\text{Re}(\text{NO})(\text{PPh}_3)(\text{PRH})$

Bill D. Zwick, Michael A. Dewey, D. Andrew Knight, William E. Buhro, Atta M. Arif, and J. A. Gladysz\*

Department of Chemistry, University of Utah, Salt Lake City, Utah 84112

Received February 20, 1992

Reactions of  $(\eta^5\text{-C}_5\text{H}_5)\text{Re}(\text{NO})(\text{PPh}_3)(\text{X})$  (X = OTs (OSO<sub>2</sub>-*p*-C<sub>6</sub>H<sub>4</sub>CH<sub>3</sub>), OTf (OSO<sub>2</sub>CF<sub>3</sub>)) with PRH<sub>2</sub> (a, R = Ph; b, R = Me; c, *t*-Bu) give the primary phosphine complexes  $[(\eta^5\text{-C}_5\text{H}_5)\text{Re}(\text{NO})(\text{PPh}_3)(\text{PRH}_2)]^+\text{X}^-$  (2a<sup>+</sup>TsO<sup>-</sup>, 2b<sup>+</sup>TfO<sup>-</sup>, 2c<sup>+</sup>TfO<sup>-</sup>; 89–96%). Reactions of 2a<sup>+</sup>c<sup>+</sup>X<sup>-</sup> with *t*-BuOK<sup>+</sup> give the phosphido complexes  $(\eta^5\text{-C}_5\text{H}_5)\text{Re}(\text{NO})(\text{PPh}_3)(\text{PRH})$  (4a–c; 63–98%). Reactions of 4c with TfOH and HCl gas give 2c<sup>+</sup>TfO<sup>-</sup> and 2c<sup>+</sup>Cl<sup>-</sup> (62–89%). NMR data show that 2c<sup>+</sup>TfO<sup>-</sup> preferentially adopts a solution RePRH<sub>2</sub> conformation that places the *tert*-butyl group in the interstice between the cyclopentadienyl and small nitrosyl ligands. An analogous conformation is found in crystalline 2c<sup>+</sup>Cl<sup>-</sup>·(CH<sub>2</sub>Cl)<sub>0.5</sub> (orthorhombic, *Pbca*, *a* = 15.265 (3) Å, *b* = 18.698 (5) Å, *c* = 19.796 (5) Å, *Z* = 8), which also exhibits a P···H···Cl hydrogen bond (H···Cl 2.90 Å). NMR, IR, and conductance properties indicate an identical interaction in solution. NMR data show that 4a,b exist as 50:50 and 89:11 mixtures of Re,P configurational diastereomers that interconvert with Δ*G*<sup>‡</sup> of 11.5 (4a) and 13.5 (4b, minor → major) kcal/mol. Reaction of 4c and MeOTf gives (*RS*,*SR*)- $[(\eta^5\text{-C}_5\text{H}_5)\text{Re}(\text{NO})(\text{PPh}_3)(\text{P}(t\text{-Bu})\text{MeH})]^+\text{TfO}^-$  (95%) in >98% diastereomeric excess (monoclinic, *P2*<sub>1</sub>/*c*, *a* = 11.499 (1) Å, *b* = 9.227 (1) Å, *c* = 30.399 (1) Å, β = 100.53 (1)°, *Z* = 4).

The synthesis, structure, and dynamic and chemical properties of transition-metal terminal phosphido complexes have continued to attract the attention of numerous researchers.<sup>1–3</sup> In particular, we have been conducting an

extensive study of chiral, coordinatively saturated, pyramidal, rhenium phosphido complexes of the general formula  $(\eta^5\text{-C}_5\text{H}_5)\text{Re}(\text{NO})(\text{PPh}_3)(\text{PXX}')$ .<sup>4–8</sup> These com-

(1) (a) Buhro, W. E.; Chisholm, M. H.; Martin, J. D.; Huffman, J. C.; Foltz, K.; Streib, W. E. *J. Am. Chem. Soc.* 1989, 111, 8149. (b) Vaughn, G. A.; Hillhouse, G. L.; Rheingold, A. L. *Organometallics* 1989, 8, 1760. (c) Dick, D. G.; Stephan, D. W. *Ibid.* 1991, 10, 2811. (d) Brombach, H.; Niecke, E.; Nieger, M. *Ibid.* 1991, 10, 3949. (e) Barre, C.; Kubicki, M. M.; Leblanc, J.-C.; Moise, C. *Inorg. Chem.* 1990, 29, 5244. (f) Bonnet, G.; Kubicki, M.; Moise, C.; Lazzaroni, R.; Salvadori, P.; Vitulli, G. *Organometallics* 1992, 11, 964. (g) Blenkiron, P.; Lavender, M. H.; Morris, M. J. *J. Organomet. Chem.* 1992, 426, C28.

(2) Fryzuk, M. D.; Joshi, K.; Chadha, R. K.; Rettig, S. J. *J. Am. Chem. Soc.* 1991, 113, 8724 and references therein.

(3) (a) Crisp, G. T.; Salem, G.; Wild, S. B.; Stephens, F. S. *Organometallics* 1989, 8, 2360. (b) Hey, E.; Willis, A. C.; Wild, S. B. *Z. Naturforsch.* 1989, 44b, 1041.

(4) (a) Buhro, W. E.; Georgiou, S.; Hutchinson, J. P.; Gladysz, J. A. *J. Am. Chem. Soc.* 1985, 107, 3346. (b) Buhro, W. E.; Zwick, B. D.; Georgiou, S.; Hutchinson, J. P.; Gladysz, J. A. *Ibid.* 1988, 110, 2427.

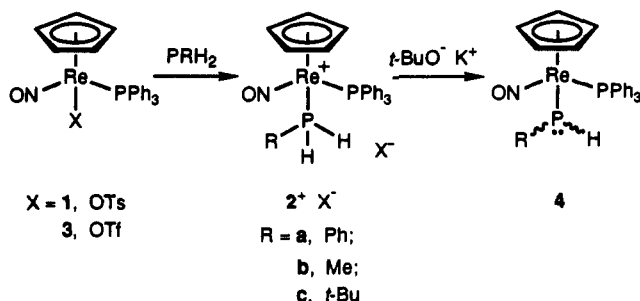
(5) Buhro, W. E.; Gladysz, J. A. *Inorg. Chem.* 1985, 24, 3505.

(6) Zwick, B. D.; Arif, A. M.; Patton, A. T.; Gladysz, J. A. *Angew. Chem., Int. Ed. Engl.* 1987, 26, 910.

(7) Buhro, W. E.; Arif, A. M.; Gladysz, J. A. *Inorg. Chem.*, 1989, 28, 3837.

(8) (a) Buhro, W. E., Ph.D. Thesis, UCLA, 1985. (b) Zwick, B. D., Ph.D. Thesis, University of Utah, 1987.

Scheme I. Synthesis of Rhenium Primary Phosphine and Phosphido Complexes



pounds are readily available in optically pure form and have been used as structural templates for novel asymmetric catalysts.<sup>6</sup>

In previous full papers, we have detailed our data on symmetrically substituted secondary phosphido complexes  $(\eta^5\text{-C}_5\text{H}_5)_2\text{Re}(\text{NO})(\text{PPh}_3)(\text{PR}_2)$  ( $\text{R} = \text{alkyl, aryl}$ )<sup>4b</sup> and functionalized phosphido complexes  $(\eta^5\text{-C}_5\text{H}_5)_2\text{Re}(\text{NO})(\text{PPh}_3)(\text{PXX}')$  ( $\text{X}$  and/or  $\text{X}' = \text{heterosubstituent}$ ).<sup>7</sup> Complementary studies involving the corresponding neutral amido and cationic amine complexes have also been reported.<sup>9,10</sup> In this paper, we describe (1) high-yield syntheses of the primary phosphine complexes  $[(\eta^5\text{-C}_5\text{H}_5)_2\text{Re}(\text{NO})(\text{PPh}_3)(\text{PRH}_2)]^+\text{X}^-$  and phosphido complexes  $(\eta^5\text{-C}_5\text{H}_5)_2\text{Re}(\text{NO})(\text{PPh}_3)(\text{PRH})$ , (2) structural analyses of each class of compounds, including hydrogen bonding interactions in the former, (3) dynamic properties of the phosphido complexes, which exhibit extremely low phosphorus inversion barriers, and (4) the highly diastereoselective methylation of a phosphido complex, and other stereoselective reactions. A small portion of this work has been communicated.<sup>5</sup>

## Results

### 1. Synthesis of Primary Phosphine Complexes.

Reactions of secondary phosphines,  $\text{PR}_2\text{H}$ , and appropriate neutral rhenium precursors  $(\eta^5\text{-C}_5\text{H}_5)_2\text{Re}(\text{NO})(\text{PPh}_3)(\text{X})$  have previously been shown to give the cationic bis(phosphine) complexes  $[(\eta^5\text{-C}_5\text{H}_5)_2\text{Re}(\text{NO})(\text{PPh}_3)(\text{PR}_2\text{H})]^+\text{X}^-$ .<sup>4</sup> Accordingly, reaction of the tosylate complex  $(\eta^5\text{-C}_5\text{H}_5)_2\text{Re}(\text{NO})(\text{PPh}_3)(\text{OTs})$  (1)<sup>11,12</sup> and the primary phosphine  $\text{PPh}_2$  ( $\text{CH}_2\text{Cl}_2$ , 2 days) gave the phenylphosphine complex  $[(\eta^5\text{-C}_5\text{H}_5)_2\text{Re}(\text{NO})(\text{PPh}_3)(\text{PPh}_2)]^+\text{TsO}^-$  ( $2\text{a}^+\text{TsO}^-$ ) in 94% yield after workup (Scheme I). Similar reactions of the triflate complex  $(\eta^5\text{-C}_5\text{H}_5)_2\text{Re}(\text{NO})(\text{PPh}_3)(\text{OTf})$  (3)<sup>11,12</sup> with methylphosphine and *tert*-butylphosphine gave the primary phosphine complexes  $[(\eta^5\text{-C}_5\text{H}_5)_2\text{Re}(\text{NO})(\text{PPh}_3)(\text{PMeH}_2)]^+\text{TfO}^-$  ( $2\text{b}^+\text{TfO}^-$ ) and  $[(\eta^5\text{-C}_5\text{H}_5)_2\text{Re}(\text{NO})(\text{PPh}_3)(\text{P}(t\text{-Bu})\text{H}_2)]^+\text{TfO}^-$  ( $2\text{c}^+\text{TfO}^-$ ) in 96% and 89% yields, respectively.

Complexes  $2\text{a-c}^+\text{X}^-$  were canary yellow powders or crystals and stable in air for a minimum of 6 years. They were characterized by microanalysis (Experimental Section) and IR and NMR ( $^1\text{H}$ ,  $^{13}\text{C}$ ,  $^{31}\text{P}$ ) spectroscopy (Table I). Most spectroscopic features were similar to those reported for the corresponding secondary phosphine com-

plexes.<sup>4</sup> The  $^{31}\text{P}\{^1\text{H}\}$  NMR spectra showed AX patterns arising from coupled  $\text{PPh}_3$  and  $\text{PRH}_2$  ligands. Both  $^1\text{H}$  and  $^{31}\text{P}$  NMR spectra exhibited large diagnostic  $^1J_{\text{HP}}$  values (368–411 Hz). The diastereotopic  $\text{PH}_2$  protons gave separate  $^1\text{H}$  NMR resonances, with the chemical shift differences in  $2\text{a}^+\text{TsO}^-$  and  $2\text{c}^+\text{TfO}^-$  being particularly pronounced ( $\Delta\delta$  1.76–1.73). The IR spectra of  $2\text{a-c}^+\text{X}^-$  showed the expected  $\nu_{\text{PH}}$  (2329–2345  $\text{cm}^{-1}$ , KBr).

The optically active *tert*-butylphosphine complex  $(-)(S)\text{-}2\text{c}^+\text{TfO}^-$ ,  $[\alpha]_{\text{D}}^{25} -141^\circ$ , was prepared from the optically active triflate complex  $(-)(S)\text{-}3^{11,13}$  by a procedure similar to that used for the racemate. The absolute configuration, corresponding to retention of configuration, was assigned by analogy to other substitution reactions of optically active  $3^{11}$  and from ORD and CD spectra (Experimental Section) utilizing criteria described earlier.<sup>11,14</sup>

### 2. Solution Structures of Phosphine Complexes.

To aid in the interpretation of phenomena described below, the structure of *tert*-butylphosphine complex  $2\text{c}^+\text{TfO}^-$  was probed by NMR spectroscopy. It has been shown that in the closely related alkyl complexes  $(\eta^5\text{-C}_5\text{H}_5)\text{M}(\text{L})(\text{PPh}_3)(\text{CH}_2\text{R})$ , the  $^3J_{\text{HP}}$  values of the diastereotopic  $\text{CH}_2$  protons exhibit a Karplus-type dependence upon the  $\text{M-CH}_2\text{R}$  conformation.<sup>15,16</sup> We anticipated that a similar relationship would hold for the primary phosphine complexes  $2\text{a-c}^+\text{X}^-$ , with maximal  $^3J_{\text{HP}}$  at  $\text{Ph}_3\text{P-Re-P-H}$  torsion angles of  $0^\circ$  and  $180^\circ$  and minimal  $^3J_{\text{HP}}$  at torsion angles of  $\pm 90^\circ$ .<sup>17</sup>

Hence,  $^1\text{H}$  NMR spectra of  $2\text{c}^+\text{TfO}^-$  were recorded between 248 and 323 K in  $\text{CDCl}_3$ . The downfield phosphorus-bound proton ( $\delta$  6.48) did not show any resolvable  $^3J_{\text{HP}}$  (digital resolution, 0.30 Hz). The upfield PH proton ( $\delta$  4.72) exhibited a  $^3J_{\text{HP}}$  that varied nonlinearly between 6.7 and 7.3 Hz,<sup>8b</sup> with an average of 7.0 Hz. Analogous trends were evident in the  $^1\text{H}$  NMR data for  $2\text{a}^+\text{TsO}^-$  and  $2\text{b}^+\text{TfO}^-$  (Table I). The downfield PH protons ( $\delta$  7.60, 5.83) exhibited very small  $^3J_{\text{HP}}$  ( $\leq 0.8$  Hz), whereas the upfield PH protons ( $\delta$  5.87, 5.03) gave larger  $^3J_{\text{HP}}$  (5.4, 5.0 Hz).

Next,  $2\text{c}^+\text{TfO}^-$  was subjected to a difference  $^1\text{H}$  NOE experiment.<sup>15b,16,18</sup> Upon irradiation of the cyclopentadienyl ligand  $^1\text{H}$  NMR resonance (65%), enhancements were observed in the downfield PH proton (1.0%), the ortho  $\text{PPh}_3$  ligand protons (1.3%), and the *tert*-butyl protons (0.1%). The upfield PH proton exhibited no enhancement. The interstice between the cyclopentadienyl and small nitrosyl ligand is known from a variety of data to be the most spacious<sup>10b,c</sup> and thus should best accommodate the phosphorus *tert*-butyl substituent. Hence,

(13) Absolute configurations are assigned by a modification of the Cahn-Ingold-Prelog priority rules in which the cyclopentadienyl ligand is considered to be pseudoatom of atomic number 30. This gives the priority sequence  $\eta^5\text{-C}_5\text{H}_5 > \text{PPh}_3 > \text{PRH}_2 > \text{PRH} > \text{OTf} > \text{NO}$ . See: Stanley, K.; Baird, M. C. *J. Am. Chem. Soc.* 1975, 97, 6598. Sloan, T. E. *Top. Stereochem.* 1981, 12, 1. Lecomte, C.; Dusausoy, Y.; Protas, J.; Tirouflet, J.; Dormand, J. *J. Organomet. Chem.* 1974, 73, 67. In compounds with rhenium and phosphorus stereocenters, the rhenium configuration is specified first. Note that the designations employed for the diastereotopic PH protons of  $2\text{a-c}^+\text{X}^-$ ,  $\text{H}_R$  and  $\text{H}_S$ , depend upon the configuration at rhenium. Thus, they are valid only for the arbitrary choice of enantiomer used in the schemes and figures of this paper.

(14) (a) Merrifield, J. H.; Strouse, C. E.; Gladysz, J. A. *Organometallics* 1982, 1, 1204. (b) Buhro, W. E.; Wong, A.; Merrifield, J. H.; Lin, G.-Y.; Constable, A. G.; Gladysz, J. A. *Ibid.* 1983, 2, 1852.

(15) (a) Stanley, K.; Baird, M. C. *J. Am. Chem. Soc.* 1975, 97, 4292. (b) Hunter, B. K.; Baird, M. C. *Organometallics* 1985, 4, 1481.

(16) (a) Davies, S. G.; Dordor-Hedgecock, I. M.; Sutton, K. H.; Whittaker, M. *J. Am. Chem. Soc.* 1987, 109, 5711. (b) Seeman, J. I.; Davies, S. G. *Ibid.* 1985, 107, 6522.

(17) Gorenstein, D. G. *Phosphorus-31 NMR, Principles and Applications*; Academic Press: Orlando, 1984; pp 43–47.

(18) Neuhaus, D.; Williamson, M. *The Nuclear Overhauser Effect in Structural and Conformational Analyses*; VCH: New York, 1989; Chapter 7.

(9) (a) Dewey, M. A.; Bakke, J. M.; Gladysz, J. A. *Organometallics* 1990, 9, 1349. (b) Dewey, M. A.; Knight, D. A.; Klein, D. P.; Arif, A. M.; Gladysz, J. A. *Inorg. Chem.* 1991, 30, 4995.

(10) (a) Dewey, M. A.; Gladysz, J. A. *Organometallics* 1990, 9, 1351. (b) Dewey, M. A.; Arif, A. M.; Gladysz, J. A. *J. Chem. Soc., Chem. Commun.* 1991, 712. (c) Dewey, M. A.; Knight, D. A.; Arif, A. M.; Gladysz, J. A. *Chem. Ber.* 1992, 125, 815.

(11) Merrifield, J. H.; Fernández, J. M.; Buhro, W. E.; Gladysz, J. A. *Inorg. Chem.* 1984, 23, 4022.

(12) Abbreviations: (a) OTs =  $\text{OSO}_2\text{-}p\text{-C}_6\text{H}_4\text{CH}_3$ . (b) OTf =  $\text{OSO}_2\text{C-F}_3$ .

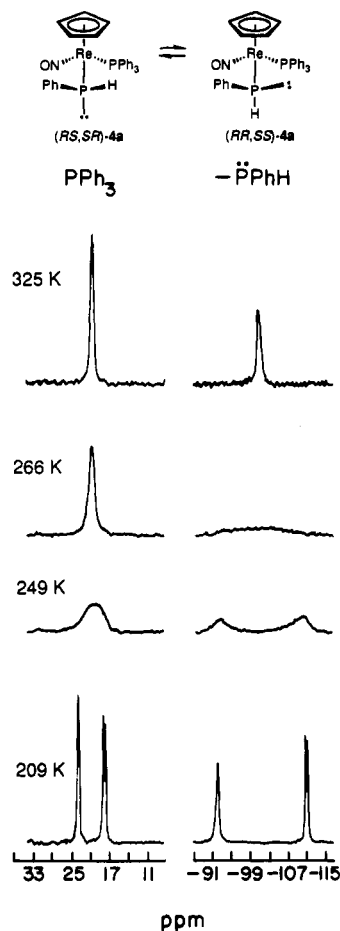
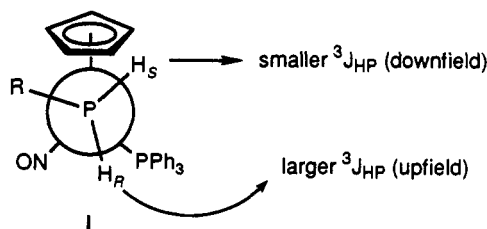


Figure 1. Variable-temperature  $^{31}\text{P}\{^1\text{H}\}$  NMR spectra of  $(\eta^5\text{-C}_5\text{H}_5)\text{Re}(\text{NO})(\text{PPh}_3)(\dot{\text{P}}\text{PhH})$  (4a) in THF.

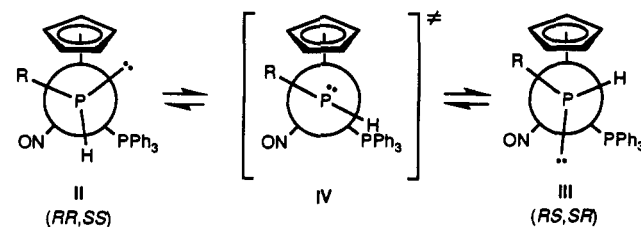
these data were interpreted as indicating a very large equilibrium concentration of the  $\text{Re-PRH}_2$  rotamer I, in which  $\text{H}_\text{S}$  and  $\text{H}_\text{R}$  would be the downfield and upfield PH protons, respectively.<sup>13</sup>



**3. Synthesis of Primary Phosphido Complexes.** The secondary phosphine complexes  $[(\eta^5\text{-C}_5\text{H}_5)\text{Re}(\text{NO})(\text{PPh}_3)(\text{PR}_2\text{H})]^+\text{X}^-$  are readily deprotonated to the corresponding secondary pyramidal phosphido complexes.<sup>4</sup> Hence, the primary phosphine complexes  $2\text{a-c}^+\text{X}^-$  were treated with  $t\text{-BuO}^-\text{K}^+$  (THF, 25 °C). Workup gave the orange, air-sensitive primary phosphido complexes  $(\eta^5\text{-C}_5\text{H}_5)\text{Re}(\text{NO})(\text{PPh}_3)(\dot{\text{P}}\text{RH})$  (4a-c) in 63–98% yields (Scheme I). Complexes 4a-c were characterized analogously to  $2^+\text{X}^-$  (Table I) and also by UV spectroscopy (Experimental Section). Most NMR and IR features were similar to those reported earlier for the secondary phosphido complexes.<sup>4</sup> Both  $^1\text{H}$  and  $^{31}\text{P}$  NMR spectra exhibited large  $^1J_{\text{HP}}$  (176–209 Hz). The IR  $\nu_{\text{PH}}$  values ( $\text{KBr}$ , 2255–2281  $\text{cm}^{-1}$ ) were somewhat lower than those of  $2^+\text{X}^-$ .

The unsymmetrically-substituted phosphido groups in 4a-c constitute stereocenters. Thus, each compound can in principle exist as two  $\text{Re}, \dot{\text{P}}$  configurational diastereomers. Accordingly, low-temperature  $^1\text{H}$  and  $^{31}\text{P}$  NMR spectra in THF or THF- $d_3$  (Table I and Figure 1) showed

Scheme II. Interconversion of Diastereomers of Phosphido Complexes  $(\eta^5\text{-C}_5\text{H}_5)\text{Re}(\text{NO})(\text{PPh}_3)(\dot{\text{P}}\text{RH})$  (4)



the phenylphosphido complex 4a to be a  $(50 \pm 2):(50 \pm 2)$  mixture of diastereomers. A solid-state IR spectrum gave doubled absorptions, suggesting the cocrystallization of both diastereomers.

Similarly, the methylphosphido complex 4b was a  $(89 \pm 2):(11 \pm 2)$  mixture of diastereomers, as assayed by  $^1\text{H}$  and  $^{31}\text{P}$  NMR spectroscopy in toluene- $d_6$  at  $-20$  °C. These data gave a  $\Delta G$  value of 1.1 kcal/mol. However, the *tert*-butylphosphido complex 4c showed only one set of resonances at temperatures as low as  $-100$  °C. Further,  $^1\text{H}$  NMR spectra recorded at 5-deg intervals between 20 and  $-100$  °C in THF- $d_3$  showed no broadening of the cyclopentadienyl resonance. The deprotonation of  $2\text{c}^+\text{TfO}^-$  in THF- $d_3$  by  $n\text{-BuLi}$  was monitored by  $^{31}\text{P}$  NMR spectroscopy at  $-98$  °C. Also, a crystal of 4c was dissolved in THF- $d_3$  that had been cooled to  $-98$  °C, and a  $^1\text{H}$  NMR spectrum was immediately recorded. In each experiment, only one set of resonances was observed. Thus, 4c was presumed to be diastereomerically homogeneous.

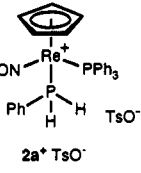
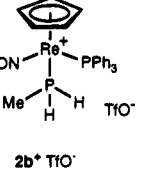
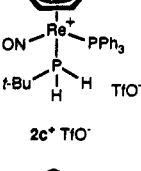
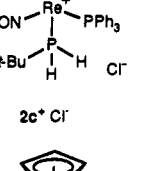
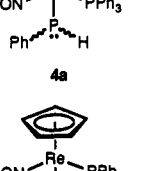
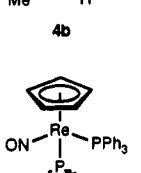
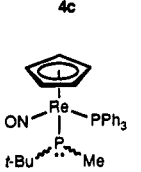
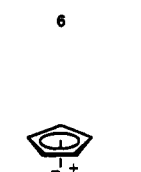
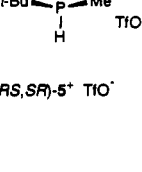
The optically active *tert*-butylphosphine complex  $(-)(S)\text{-}2\text{c}^+\text{TfO}^-$  was converted to the optically active *tert*-butylphosphido complex  $(-)(S)\text{-}4\text{c}$ ,  $[\alpha]_{589}^{25} -125^\circ$ , by a procedure analogous to that used for the racemate. This ligand-based reaction was assumed to proceed with retention of configuration at rhenium, as supported by ORD and CD spectral data (Experimental Section). The optical rotation of  $(-)(S)\text{-}4\text{c}$  showed negligible change after several days in THF at room temperature ( $[\alpha]_{589}^{25} -122^\circ$ ). Analogous optically active, symmetrically-substituted phosphido complexes behave similarly.<sup>4b</sup> Thus, there must be an appreciable barrier to inversion of configuration at rhenium in 4a-c.

**4. Dynamic and Structural Properties of Phosphido Complexes.** When NMR samples of the phenylphosphido complex 4a were warmed, the  $\text{PPh}_3$  and  $\dot{\text{P}}\text{PhH}$   $^{31}\text{P}$  resonances of the two diastereomers coalesced. The cyclopentadienyl and  $\dot{\text{P}}\text{H}$   $^1\text{H}$  NMR resonances behaved similarly. Representative spectra are shown in Figure 1, and data are summarized in Table II. Standard analyses<sup>19</sup> gave a  $\Delta G^*_{\text{T}(c)}$  of only 11.5–11.6 kcal/mol for diastereomer interconversion. In view of the optical stability of other phosphido complexes noted above, this process must involve inversion of configuration at phosphorus.

When NMR samples of the methylphosphido complex 4b were warmed, the cyclopentadienyl and methyl  $^1\text{H}$  resonances similarly coalesced. Representative spectra are shown in Figure 2. As summarized in Table II, the data establish a  $\Delta G^*_{\text{T}(c)}$  of 13.5–13.6 kcal/mol for the conversion of the minor diastereomer to the major diastereomer. The  $\Delta G^*_{\text{T}(c)}$  values calculated for the conversion of the major diastereomer to the minor diastereomer are, as expected from the  $\Delta G$  given above, ca. 1.1 kcal/mol greater.

On the basis of previous studies of analogous secondary phosphido and primary amido complexes,<sup>4b,10b,c</sup> the

Table I. Spectroscopic Characterization of New Rhenium Phosphine and Phosphido Complexes

	IR, cm <sup>-1</sup> (KBr)	<sup>1</sup> H NMR, <sup>a</sup> δ	<sup>31</sup> P{ <sup>1</sup> H} NMR, <sup>b</sup> ppm	<sup>13</sup> C{ <sup>1</sup> H} NMR, <sup>c</sup> ppm
	3160-2840 m, ν <sub>PH</sub> 2329 w, ν <sub>NO</sub> 1699 vs, 1586 w, 1573 w, 1495 w, 1481 m, 1436 s, 1311 w, 1203 s vbr, 1161 m, 1119 s, 1095 s, 1073 m, 1033 s, 1012 s, 998 m, 925 m, 908 m, 858 m, 816 m, 741 m, 695 s, 679 s	7.69 (d, <sup>3</sup> J <sub>HH</sub> = 8.1, 2 H), 7.60 (ddd, <sup>1</sup> J <sub>HP</sub> = 411, <sup>2</sup> J <sub>HH</sub> = 3.8, <sup>3</sup> J <sub>HP</sub> = 0.8, PH <sub>2</sub> ), 7.54-7.27 (m, 20 H), 7.09 (d, <sup>3</sup> J <sub>HH</sub> = 7.8, 2 H), 5.87 (ddd, <sup>1</sup> J <sub>HP</sub> = 393, <sup>2</sup> J <sub>HH</sub> = 4.4, <sup>3</sup> J <sub>HP</sub> = 5.4, PH <sub>2</sub> ), 5.61 (s, C <sub>6</sub> H <sub>5</sub> ), 2.30 (s, CH <sub>3</sub> ) <sup>d</sup>	15.87 (d, <i>J</i> = 14.9, PPh <sub>3</sub> ), -70.73 (d, <i>J</i> = 14.4, PH <sub>2</sub> Ph) <sup>d,e</sup>	OTs at 146.13 (s, i), 139.40 (s, o), 129.13 (s, m), 126.63 (s, p), 21.41 (s, CH <sub>3</sub> ); PPh <sub>3</sub> at 134.09 (d, <sup>2</sup> J = 11.1, o), 132.90 (d, <sup>1</sup> J = 57.7, i), 132.36 (d, <sup>4</sup> J = 2.5, p), 130.10 (d, <sup>3</sup> J = 11.0, m); PPhH <sub>2</sub> at 133.93 (d, <sup>2</sup> J = 11.8, o), 132.06 (d, <sup>4</sup> J = 2.6, p), 129.88 (d, <sup>3</sup> J = 11.9, m); 92.47 (s, C <sub>6</sub> H <sub>5</sub> ) <sup>d</sup>
	3015 m, 3089 m, 3001 w, ν <sub>PH</sub> 2337 br w, ν <sub>NO</sub> 1695 vs, 1587 w, 1575 w, 1482 m, 1417 m, 1280 vs, ν <sub>NO</sub> 1258 vs, 1223 m, 1151 s, 1095 s, 1031 vs, 985 m, 751 m, 698 s, 636 vs	7.55-7.51 (m, 9 H), 7.33-7.25 (m, 6 H), 5.83 (dm, <sup>1</sup> J <sub>HP</sub> = 392.8, <sup>2</sup> J <sub>HH</sub> = 2.4, <sup>h</sup> PH <sub>2</sub> ), 5.54 (d, <sup>3</sup> J <sub>HP</sub> = 0.6, C <sub>6</sub> H <sub>5</sub> ), 5.03 (dm, <sup>1</sup> J <sub>HP</sub> = 388.1, <sup>3</sup> J <sub>HP</sub> = 5.0, <sup>h</sup> <sup>2</sup> J <sub>HH</sub> = 2.8, <sup>h</sup> PH <sub>2</sub> ), 1.71 (ddd, <sup>2</sup> J <sub>HP</sub> = 12.8, <sup>3</sup> J <sub>HH</sub> = 6.5, <sup>3</sup> J <sub>HH</sub> = 6.2, CH <sub>3</sub> ) <sup>d</sup>	14.67 (d, <i>J</i> = 17.2, PPh <sub>3</sub> ), -101.02 (d, <sup>h</sup> <i>J</i> = 17.2, PH <sub>2</sub> Me) <sup>d</sup>	PPh <sub>3</sub> at 133.33 (d, <sup>2</sup> J = 11.0, o), 132.46 (dd, <sup>1</sup> J = 57.2, <sup>3</sup> J = 1.8, i), 131.97 (d, <sup>4</sup> J = 2.4, p), 129.15 (d, <sup>3</sup> J = 11.1, m); 91.70 (s, C <sub>6</sub> H <sub>5</sub> ), 5.88 (dd, <sup>1</sup> J = 41.3, <sup>3</sup> J = 1.6, CH <sub>3</sub> ) <sup>d,h</sup>
	3404 w, 3081 m, 2958 m, 2902 w, 2845 w, ν <sub>PH</sub> 2345 m, ν <sub>NO</sub> 1715 vs, 1586 w, 1574 w, 1482 m, 1436 s, 1369 m, ν <sub>NO</sub> 1267 vs, 1225 s, 1152 s, 1095 s, 1031 vs, 999 m, 905 s, 855 m, 749 s, 697 s	7.54-7.52 (m, 9 H), 7.30-7.23 (m, 6 H), 6.48 (dd, <sup>1</sup> J <sub>HP</sub> = 382.5, <sup>2</sup> J <sub>HH</sub> = 4.7, PH <sub>2</sub> ), 5.57 (s, C <sub>6</sub> H <sub>5</sub> ), 4.72 (ddd, <sup>1</sup> J <sub>HP</sub> = 368.3, <sup>3</sup> J <sub>HP</sub> = 7.3, <sup>2</sup> J <sub>HH</sub> = 4.7, PH <sub>2</sub> ), 1.23 (d, <sup>3</sup> J <sub>HP</sub> = 18.1, 3 CH <sub>3</sub> ) <sup>j</sup>	17.20 (d, <i>J</i> = 15.0, PPh <sub>3</sub> ), -35.40 (d, <sup>h</sup> <i>J</i> = 15.0, PH <sub>2</sub> R) <sup>j</sup>	PPh <sub>3</sub> at 133.11 (d, <sup>2</sup> J = 10.6, o), 131.70 (dd, <sup>1</sup> J = 57.8, <sup>3</sup> J = 1.3, i), 131.60 (d, <sup>4</sup> J = 3.0, p), 129.26 (d, <sup>3</sup> J = 10.4, m); 91.84 (s, C <sub>6</sub> H <sub>5</sub> ), 32.81 (dd, <sup>1</sup> J = 39.5, <sup>3</sup> J = 1.4, PCC <sub>3</sub> ), 29.42 (d, <sup>2</sup> J = 4.2, 3 CH <sub>3</sub> ) <sup>j,k</sup>
	ν <sub>PH</sub> 2311 m, ν <sub>NO</sub> 1684 vs	7.68 (dd, <sup>1</sup> J <sub>HP</sub> = 393.0, <sup>2</sup> J <sub>HH</sub> = 4.2, PH <sub>2</sub> ), 7.54-7.51 (m, 6 H), 7.37-7.26 (m, 9 H), 5.74 (s, C <sub>6</sub> H <sub>5</sub> ), 4.67 (ddd, <sup>1</sup> J <sub>HP</sub> = 365.2, <sup>3</sup> J <sub>HP</sub> = 7.6, <sup>2</sup> J <sub>HH</sub> = 4.5, PH <sub>2</sub> ), 1.27 (d, <sup>3</sup> J <sub>HP</sub> = 17.9, 3 CH <sub>3</sub> ) <sup>j</sup>	18.19 (d, <i>J</i> = 14.4, PPh <sub>3</sub> ), -37.86 (d, <i>J</i> = 14.4, PH <sub>2</sub> R) <sup>j</sup>	PPh <sub>3</sub> at 133.05 (d, <sup>2</sup> J = 11.0, o), 131.74 (d, <sup>1</sup> J = 57.2, i), 131.31 (d, <sup>4</sup> J = 2.8, p), 129.04 (d, <sup>3</sup> J = 10.0, m); 91.11 (s, C <sub>6</sub> H <sub>5</sub> ), 32.76 (d, <sup>1</sup> J = 38.2, PCC <sub>3</sub> ), 29.60 (d, <sup>2</sup> J = 3.9, 3 CH <sub>3</sub> ) <sup>j</sup>
	3052 m, ν <sub>PH</sub> 2281/2255 m, ν <sub>NO</sub> 1654/1627 vs, 1580 m, 1572 m, 1480 m, 1433 s, 1309 w, 1182 m, 1160 w, 1093 m, 1067 w, 1025 w, 998 m, 888 w, 857 m, 820 m, 751 m, 742 m, 695 s	7.63-7.27 (m, 17 H), 7.09-6.99 (m, 2 H), 6.95-6.87 (m, 1 H), 5.19/4.86 (2 s, C <sub>6</sub> H <sub>5</sub> ), 3.74/3.34 (dd/d, <sup>1</sup> J <sub>PH</sub> 209/199, <sup>3</sup> J <sub>PH</sub> ca. 10/<2, PH) <sup>l,m</sup>	24.22/18.72 (s/d, <i>J</i> = <2/15.4, PPh <sub>3</sub> ), -91.84/-110.68 (s/d, <sup>h</sup> <i>J</i> = <2/15.4, PPHH) <sup>l,n</sup>	PPh <sub>3</sub> at 137.43 (d, <sup>2</sup> J = 53.2, i), 135.08 (dd, <sup>2</sup> J = 10.4, <sup>4</sup> J = 2.7, o), 131.22 (d, <sup>4</sup> J = 2.5, p), 129.25 (d, <sup>3</sup> J = 10.3, m); PPHH at 133.75 (d, <sup>2</sup> J = 14.8, o), 128.10 (d, <sup>3</sup> J = 4.0, m), 125.32 (s, p); 91.72 (s, C <sub>6</sub> H <sub>5</sub> ) <sup>l,o</sup>
	3233 w, 3115 w, 3053 w, 2951 w, 2896 w, ν <sub>PH</sub> 2260 m, ν <sub>NO</sub> 1631 vs, 1584 m, 1572 m, 1480 m, 1434 s, 1090 m, 998 m, 816 m, 751 m, 697 s	7.56-7.49 (m, 6 H), 7.02-6.92 (m, 9 H), 4.57/4.54 (d/s, major/minor, <sup>3</sup> J <sub>HP</sub> = 1.4/<1, C <sub>6</sub> H <sub>5</sub> ), 3.28 (ddd, <sup>1</sup> J <sub>HP</sub> = 191.9, <sup>3</sup> J <sub>HP</sub> = 8.0, <sup>3</sup> J <sub>HH</sub> = 7.1, PH), 1.90/1.56 (2 dd, major/minor, <sup>3</sup> J <sub>HH</sub> = 6.9/6.2, <sup>2</sup> J <sub>HP</sub> = 4.0/6.2, CH <sub>3</sub> ) <sup>p,q</sup>	25.65/21.28 (2 d, major/minor, <i>J</i> = 6.5/19.1, PPh <sub>3</sub> ), -127.26/-150.42 (2 d, <sup>h</sup> major/minor, <i>J</i> = 6.4/19.1 Hz, PHMe) <sup>p,q</sup>	PPh <sub>3</sub> at 137.14 (d, <sup>1</sup> J = 53.2, i), 134.37 (dd, <sup>2</sup> J = 10.8, <sup>4</sup> J = 2.7, o), 130.66 (d, <sup>4</sup> J = 2.1, p), 128.73 (d, <sup>3</sup> J = 10.4, m); 90.98/89.83 (dd/d, major/minor, <sup>3</sup> J = 3.7/1.5, 1.5/<1, C <sub>6</sub> H <sub>5</sub> ), 9.44 (dd, <sup>1</sup> J = 26.1, <sup>3</sup> J = 3.4, CH <sub>3</sub> ) <sup>l,r</sup>
	3089 w, 3053 w, 2924 m, 2883 m, 2848 m, ν <sub>PH</sub> 2273 m, ν <sub>NO</sub> 1632 vs, 1479 s, 1435 s, 1353 m, 1178 m, 1090 s, 999 m, 913 s, 753 s, 745 s, 695 vs, 682 s, 619 m	7.60-7.54 (m, 6 H), 7.16-6.95 (m, 9 H), 4.78 (d, <sup>3</sup> J <sub>HP</sub> = 1.0, C <sub>6</sub> H <sub>5</sub> ), 3.53 (dd, <sup>1</sup> J <sub>HP</sub> = 198.0, <sup>3</sup> J <sub>HP</sub> = 10.6, PH), 1.31 (d, <sup>3</sup> J <sub>HP</sub> = 10.5, 3 CH <sub>3</sub> ) <sup>r</sup>	25.80 (br, PPh <sub>3</sub> ), -34.60 (br, <sup>h</sup> PHR) <sup>i</sup>	PPh <sub>3</sub> at 136.53 (d, <sup>4</sup> J = 53.5, i), 133.91 (d, <sup>2</sup> J = 10.2, o), 130.02 (s, p), 128.38 (s, <sup>h</sup> m); 90.79 (s, C <sub>6</sub> H <sub>5</sub> ), 34.79 (d, <sup>2</sup> J = 11.8, CH <sub>3</sub> ), 32.81 (dd, <sup>1</sup> J = 15.1, <sup>3</sup> J = 3.0, PC) <sup>r</sup>
	3252 w, 3076 w, 2954 m, 2941 m, 2928 m, 2915 m, 2888 m, 2849 m, 2205 w, ν <sub>NO</sub> 1634 vs, 1588 m, 1574 w, 1480 m, 1434 m, 1351 m, 1091 m, 820 m, 811 m, 744 m, 695 s	7.65-7.63 (m, 6 H), 7.61-7.33 (m, 9 H), 5.00/5.12 (s/d, major/minor, <sup>2</sup> J <sub>HP</sub> = <1/1.4, C <sub>6</sub> H <sub>5</sub> ), 1.10/1.17 (d/d, major/minor, <sup>3</sup> J <sub>HP</sub> = 10.4/10.4, 3 CH <sub>3</sub> ), 0.54/0.84 (d/d, major/minor, <sup>2</sup> J <sub>HP</sub> = 6.4/5.5, PCH <sub>3</sub> ) <sup>l,t</sup>	16.40/24.07 (d/s, major/minor, <i>J</i> = 29.9/<2, PPh <sub>3</sub> ), -55.84/-27.50, d/s, major/minor, <i>J</i> = 29.9/<2, 29.9/<2, PRR) <sup>l,t</sup>	PPh <sub>3</sub> (major/minor) at 136.64/136.99 (2 d, <sup>1</sup> J = 52.3/55.6, i), 134.85/134.52 (dd/d, <sup>2</sup> J = 9.5/10.4, <sup>4</sup> J = 4.0/<2, o), 130.49/130.88 (d/s, <sup>4</sup> J = 1.8/<1, p), 128.62/129.10 (2 d, <sup>3</sup> J = 10.1/10.0, m); 90.39/93.51 (s/d, <sup>2</sup> J = <2/4.3 Hz, C <sub>6</sub> H <sub>5</sub> ), 32.87/35.73 (dd/d, <sup>1</sup> J = 32.2/20.6, <sup>3</sup> J = 6.0/<2, PCC <sub>3</sub> ), 30.91/31.88 (2 d, <sup>2</sup> J = 16.0/14.6, 3 CH <sub>3</sub> ), 10.55 (d, <sup>1</sup> J = 37.1, PCH <sub>3</sub> ) <sup>l,r</sup>
	3381 w, 3113 m, 2961 m, 2993 m, 2897 w, ν <sub>PH</sub> 2258 w, ν <sub>NO</sub> 1704 vs, 1587 w, 1574 w, 1482 m, 1436 s, 1367 m, ν <sub>NO</sub> 1267 vs, 1224 s, 1153 s, 1094 s, 1032 s, 999 m, 755 m, 698 s, 637 s	7.55-7.52 (m, 9 H), 7.34-7.27 (m, 6 H), 5.53 (s, C <sub>6</sub> H <sub>5</sub> ), 5.13 (ddd, <sup>1</sup> J <sub>HP</sub> = 364.4, <sup>3</sup> J <sub>HP</sub> = 9.6, <sup>3</sup> J <sub>HH</sub> = 4.7, PH), 1.59 (dd, <sup>2</sup> J <sub>HP</sub> = 9.6, <sup>3</sup> J <sub>HH</sub> = 6.5, PCH <sub>3</sub> ), 1.19 (d, <sup>3</sup> J <sub>HP</sub> = 17.1, 3 CH <sub>3</sub> ) <sup>j</sup>	15.72 (d, <i>J</i> = 15.7, PPh <sub>3</sub> ), -2.26 (d, <i>J</i> = 15.7, PHRR) <sup>j</sup>	PPh <sub>3</sub> at 132.82 (d, <sup>2</sup> J = 10.7, o), 131.91 (dd, <sup>1</sup> J = 57.0, <sup>3</sup> J = 1.4, i), 131.60 (d, <sup>4</sup> J = 2.3, p), 129.16 (d, <sup>3</sup> J = 10.6, m); 91.60 (s, C <sub>6</sub> H <sub>5</sub> ), 34.27 (dd, <sup>1</sup> J = 38.5, <sup>3</sup> J = 2.3, PCC <sub>3</sub> ), 27.78 (d, <sup>2</sup> J = 4.3, 3 CH <sub>3</sub> ), 8.60 (d, <sup>1</sup> J = 33.3, PCH <sub>3</sub> ) <sup>j</sup>

(RS,SR)-5<sup>+</sup> TlO<sup>-</sup>

Table I (Continued)

IR, cm <sup>-1</sup> (KBr)	<sup>1</sup> H NMR, <sup>a</sup> δ	<sup>31</sup> P{ <sup>1</sup> H} NMR, <sup>b</sup> ppm	<sup>13</sup> C{ <sup>1</sup> H} NMR, <sup>c</sup> ppm
 ( <i>RR,SS</i> )-5 <sup>+</sup> TlO <sup>-</sup>	7.55–7.52 (m, 9 H), 7.34–7.27 (m, 6 H), 6.80 (q, <sup>3</sup> J <sub>HH</sub> = 6.3, 0.5PH) <sup>h</sup> , 5.55 (s, C <sub>5</sub> H <sub>5</sub> ), 1.24 (d, <sup>3</sup> J <sub>HP</sub> = 15.8, 3 CH <sub>3</sub> ), 0.99 (dd, <sup>2</sup> J <sub>HP</sub> = 10.9, <sup>3</sup> J <sub>HH</sub> = 6.3, PCH <sub>3</sub> ) <sup>j</sup>	14.47 (d, <i>J</i> = 14.0, PPh <sub>3</sub> ), -37.79 (d, <i>J</i> = 14.0, PRRR') <sup>j</sup>	PPh <sub>3</sub> at 133.85 (d, <sup>1</sup> J = 55.4, <i>i</i> ), 133.25 (d, <sup>2</sup> J = 11.0, <i>o</i> ), 131.69 ( <i>s</i> , <i>p</i> ), 129.40 (d, <sup>3</sup> J = 10.6, <i>m</i> ); 91.92 ( <i>s</i> , C <sub>5</sub> H <sub>5</sub> ), 35.04 (d, <sup>1</sup> J = 38.7, PCC <sub>3</sub> ), 28.60 (d, <sup>2</sup> J = 3.7, 3 CH <sub>3</sub> ), 6.33 (d, <sup>1</sup> J = 32.3, PCH <sub>3</sub> ) <sup>j</sup>

<sup>a</sup> At 300 MHz and ambient probe temperature and referenced to internal Si(CH<sub>3</sub>)<sub>4</sub>. All couplings are in hertz. <sup>b</sup> At 121 MHz and ambient probe temperature and referenced to external 85% H<sub>3</sub>PO<sub>4</sub>. All couplings (hertz) are to phosphorus. <sup>c</sup> At 75 MHz and ambient probe temperature and referenced to internal Si(CH<sub>3</sub>)<sub>4</sub>. All couplings (hertz) are to phosphorus. Assignments of resonances to the PPh<sub>3</sub> carbons are made as described in footnote *c* of Table I in: Buhro, W. E.; Georgiou, S.; Fernández, J. M.; Patton, A. T.; Strouse, C. E.; Gladysz, J. A. *Organometallics* 1986, 5, 956. <sup>d</sup> In CD<sub>2</sub>Cl<sub>2</sub>. <sup>e</sup> At -51 °C. <sup>f</sup> Ipso carbon resonance not observed. <sup>g</sup> <sup>31</sup>P NMR spectra (no proton decoupling) show <sup>1</sup>J<sub>PH</sub> = 398.6, 389.2 (dd, 2b<sup>+</sup>TfO<sup>-</sup>); 371 (t, 2c<sup>+</sup>TfO<sup>-</sup>); 377.6 (t, 2c<sup>+</sup>Cl<sup>-</sup>); 209/200 (d/f, 4a); 190.9/175.6 (d/d, 4b); 200 (4c). <sup>h</sup> Determined from a decoupling experiment in which the δ 1.71 resonance was irradiated. <sup>i</sup> CF<sub>3</sub> carbon resonance not observed. <sup>j</sup> In CDCl<sub>3</sub>. <sup>k</sup> The other portion of this resonance is obscured. <sup>l</sup> In THF-*d*<sub>6</sub> or THF. <sup>m</sup> At -74 °C. <sup>n</sup> At -64 °C. <sup>o</sup> At 60 °C. <sup>p</sup> In toluene-*d*<sub>6</sub>. <sup>q</sup> At -20 °C. <sup>r</sup> At -30 °C. <sup>s</sup> In C<sub>6</sub>D<sub>6</sub>. <sup>t</sup> At -25 °C.

Table II. Summary of Dynamic NMR Data for Diastereomeric Phosphido Complexes (η<sup>5</sup>-C<sub>5</sub>H<sub>5</sub>)Re(NO)(PPh<sub>3</sub>)(PMe)

compd	resonance	Δν, Hz (T, K) <sup>a</sup>	T(c), K	ΔP <sup>b</sup>	ΔG <sup>‡</sup> , <sup>c</sup> kcal/mol
4a <sup>d</sup>	<sup>1</sup> H C <sub>5</sub> H <sub>5</sub>	99.9 (194)	243	<0.02	11.5 ± 0.1
	<sup>31</sup> P PPhH	177.4 (209)	248	<0.02	11.5 ± 0.1
	<sup>31</sup> P PPh <sub>3</sub>	606.7 (209)	265	<0.02	11.6 ± 0.1
4b <sup>d</sup>	<sup>1</sup> H C <sub>5</sub> H <sub>5</sub>	8.4 (213)	258	0.865	13.5 ± 0.1
	<sup>1</sup> H Me	31.7 (213)	272	0.737	13.6 ± 0.1
6 <sup>f</sup>	<sup>1</sup> H C <sub>5</sub> H <sub>5</sub>	73.4 (223)	306	0.634	14.9 ± 0.1
	<sup>1</sup> H <i>t</i> -Bu	38.2 (223)	297	0.596	15.0 ± 0.1
					14.9 ± 0.1 <sup>e</sup>
					14.6 ± 0.1 <sup>e</sup>
					15.8 ± 0.1 <sup>e</sup>
					15.6 ± 0.1 <sup>e</sup>

<sup>a</sup> Frequency difference between the two resonances that coalesce. <sup>b</sup> ΔP = P<sub>1</sub> - P<sub>2</sub>, where P<sub>1</sub> and P<sub>2</sub> are the normalized populations of the two diastereomers, as determined by integration of the low-temperature-limit NMR spectrum. <sup>c</sup> The error limits correspond to an uncertainty of ±2 K in T(c).<sup>19</sup> <sup>d</sup> In THF or THF-*d*<sub>6</sub>. <sup>e</sup> For the conversion of the minor diastereomer to the major diastereomer. <sup>f</sup> In toluene-*d*<sub>6</sub>.

idealized structures II and III (Scheme II) are likely to represent the most stable Re-PRH rotamers of the *RR,SS* and *RS,SR* diastereomers<sup>13</sup> of 4a–c. We sought to assign configurations to each pair of diastereomers. However, their rapid interconversion precluded the type of NOE experiment conducted with 2c<sup>+</sup>TfO<sup>-</sup>. Thus, orange gem-quality prisms of 4c were grown from benzene/hexane, and X-ray data were collected as described elsewhere.<sup>8b</sup>

Refinement gave a structure exhibiting positional disorder of the *tert*-butylphosphido ligand and probable polysynthetic twinning.<sup>20</sup> As a result, a very poor structure solution was obtained (*R*<sub>w</sub> 0.17). The major component (ca. 80%) showed a Re-PRH conformation that placed the *tert*-butyl group in the interstice between the nitrosyl and cyclopentadienyl ligands, with a Ph<sub>3</sub>P-Re-P-C torsion angle of ca. 125°. The Re-PRH conformation of the minor component appeared to orient the *tert*-butyl group between the cyclopentadienyl and PPh<sub>3</sub> ligands. No PH protons were located, and diastereomer assignments were made from reactivity data and spectroscopic correlations as described below.

**5. Protonation of Phosphido Complexes.** The secondary phosphido complexes (η<sup>5</sup>-C<sub>5</sub>H<sub>5</sub>)Re(NO)(PPh<sub>3</sub>)(PR<sub>2</sub>) are extremely reactive toward electrophiles.<sup>4</sup> Thus, a benzene solution of 4c was treated with triflic acid (1.0 equiv). Workup gave the *tert*-butylphosphine complex 2c<sup>+</sup>TfO<sup>-</sup> in 62% yield (Scheme III).

(20) Bueger, M. J. *Crystal-Structure Analysis*; Wiley: New York, 1960; pp 53–68.

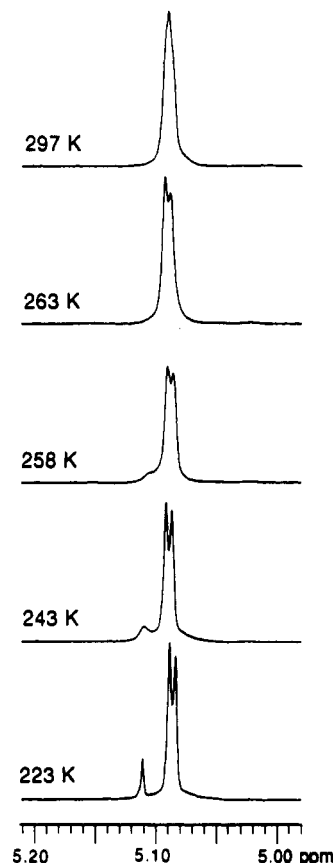


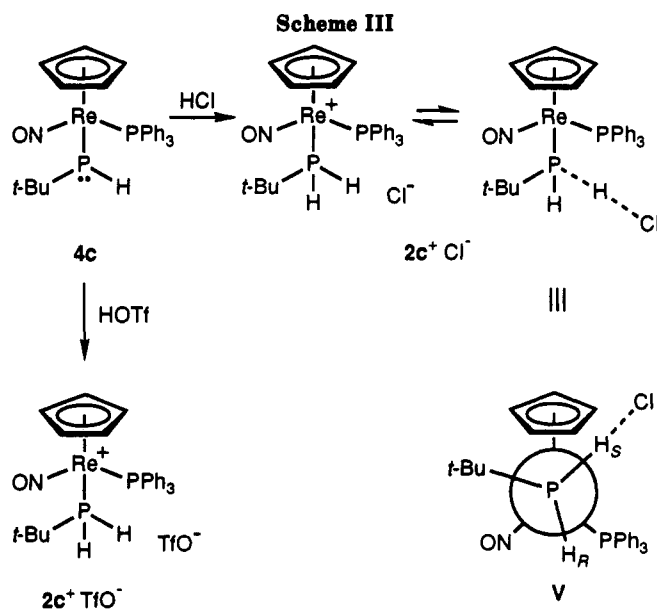
Figure 2. Variable-temperature <sup>1</sup>H NMR spectra of (η<sup>5</sup>-C<sub>5</sub>H<sub>5</sub>)Re(NO)(PPh<sub>3</sub>)(PMeH) (4b) in THF-*d*<sub>6</sub> (cyclopentadienyl resonance region).

Next, 4c and excess HCl gas were similarly reacted. Workup gave the phosphine complex 2c<sup>+</sup>Cl<sup>-</sup> as a yellow foam (89%; Scheme III). Interestingly, some spectroscopic features differed significantly from those of 2c<sup>+</sup>TfO<sup>-</sup> (Table I). For example, IR spectra showed ν<sub>PH</sub> (KBr/CHCl<sub>3</sub>: 2311/2325–2326 cm<sup>-1</sup>) that were lower than that of 2c<sup>+</sup>TfO<sup>-</sup> (KBr/CHCl<sub>3</sub>: 2345–2349/2338 cm<sup>-1</sup>). Also, the <sup>1</sup>H NMR chemical shifts of the PH protons differed by >3.00 ppm. One (δ 4.67) was very close to that of H<sub>R</sub> in 2c<sup>+</sup>TfO<sup>-</sup> (δ 4.72; see I), whereas the other (δ 7.68) was shifted 1.20 ppm downfield from H<sub>S</sub> in 2c<sup>+</sup>TfO<sup>-</sup> (δ 6.48). The <sup>3</sup>J<sub>HP</sub> were virtually unaffected, suggestive of an unperturbed Re-PRH<sub>2</sub> conformation.

The conductance (Ω<sub>M</sub>) of dichloromethane solutions of 2c<sup>+</sup>Cl<sup>-</sup> and 2c<sup>+</sup>TfO<sup>-</sup> (1.03–1.07 × 10<sup>-3</sup> M) was measured. Values of 20 and 48 Ω<sup>-1</sup> were obtained, respectively. Under comparable conditions, the carbonyl complex [(η<sup>5</sup>-C<sub>5</sub>H<sub>5</sub>)-

**Table III. Summary of Crystallographic Data for Phosphine Complexes  $[(\eta^5\text{-C}_5\text{H}_5)\text{Re}(\text{NO})(\text{PPh}_3)(\text{P}(t\text{-Bu})\text{H}_2)]^+\text{Cl}^- \cdot 0.5\text{CH}_2\text{Cl}_2$  ( $2\text{c}^+\text{Cl}^- \cdot 0.5\text{CH}_2\text{Cl}_2$ ) and  $(RS,SR)\text{-}[(\eta^5\text{-C}_5\text{H}_5)\text{Re}(\text{NO})(\text{PPh}_3)(\text{P}(t\text{-Bu})\text{MeH})]^+\text{TfO}^-$  ( $(RS,SR)\text{-}5^+\text{TfO}^-$ )**

compound	$2\text{c}^+\text{Cl}^- \cdot 0.5\text{CH}_2\text{Cl}_2$	$(RS,SR)\text{-}5^+\text{TfO}^-$
mol formula	$\text{C}_{27}\text{H}_{31}\text{ClNO}_2\text{P}_2\text{Re} \cdot 0.5\text{CH}_2\text{Cl}_2$	$\text{C}_{29}\text{H}_{33}\text{F}_3\text{NO}_4\text{P}_2\text{ReS}$
mol wt	711.66	796.798
cryst system	orthorhombic	monoclinic
space group	$Pbca$ (No. 61)	$P2_1/c$ (No. 14)
cell dimens (16 °C)		
<i>a</i> , Å	15.265 (3)	11.499 (1)
<i>b</i> , Å	18.698 (5)	9.227 (1)
<i>c</i> , Å	19.796 (5)	30.399 (1)
β, deg		100.53 (1)
<i>v</i> , Å <sup>3</sup>	5650.44	3170.90
<i>Z</i>	8	4
<i>d</i> <sub>obs</sub> , gm/cm <sup>3</sup> (22 °C)	1.66	1.67
<i>d</i> <sub>calc</sub> , gm/cm <sup>3</sup> (16 °C)	1.67	1.66
cryst dimens, mm	$0.35 \times 0.28 \times 0.15$	$0.40 \times 0.25 \times 0.12$
radiatn, Å	Mo Kα (0.71073)	Mo Kα (0.71073)
data collection method	θ-2θ	θ-2θ
scan speed, deg/min	variable, 3.0-8.0	3.0-8.0
reflms measured	4423	5721
range/indices ( <i>hkl</i> )	0,18, 0,22, 0,23	0,13, 0,10, -34,34
scan range	Kα <sub>1</sub> -1.0 to Kα <sub>2</sub> +1.0	Kα <sub>1</sub> -1.3 to Kα <sub>2</sub> +1.3
2θ limit, deg	3.0-46.0	3.0-46.0
no. of reflms between std	98	98
total unique data	4423	5602
obsd data, <i>I</i> > 3σ( <i>I</i> )	2567	3582
abs coeff, cm <sup>-1</sup>	49.78	40.96
min transmission, %	69.96	70.48
max transmission, %	99.89	99.98
no. of variables	316	391
goodness of fit	2.55	3.38
$R = \sum   F_o  -  F_c   / \sum  F_o $	0.033	0.037
$R_w = \sum   F_o  -  F_c  w^{1/2} / \sum  F_o w^{1/2}$	0.036	0.043
Δ/σ (max)	0.003	0.032
Δρ (max, eÅ <sup>-3</sup> )	0.503, 0.924 Å from Re	1.044, 1.276 Å from Re



$\text{Re}(\text{NO})(\text{PPh}_3)(\text{CO})]^+\text{BF}_4^-$ , in which there is no precedent possibility for significant cation/anion interactions, gave  $\Omega_M$  of 50–60  $\Omega^{-1}$ . Thus, solutions of  $2\text{c}^+\text{Cl}^-$  show much less conductance than those of related compounds that must be 1:1 electrolytes. The preceding data were taken as evidence for a  $\text{P}\cdots\text{H}\cdots\text{Cl}$  hydrogen bond involving the  $\text{H}_S$  proton in  $2\text{c}^+\text{Cl}^-$ , as shown in V (Scheme III).<sup>21</sup>

This structural issue was probed crystallographically. X-ray data were collected on the solvate  $2\text{c}^+\text{Cl}^- \cdot (\text{CH}_2\text{Cl}_2)_{0.5}$  as summarized in Table III. Refinement, described in the

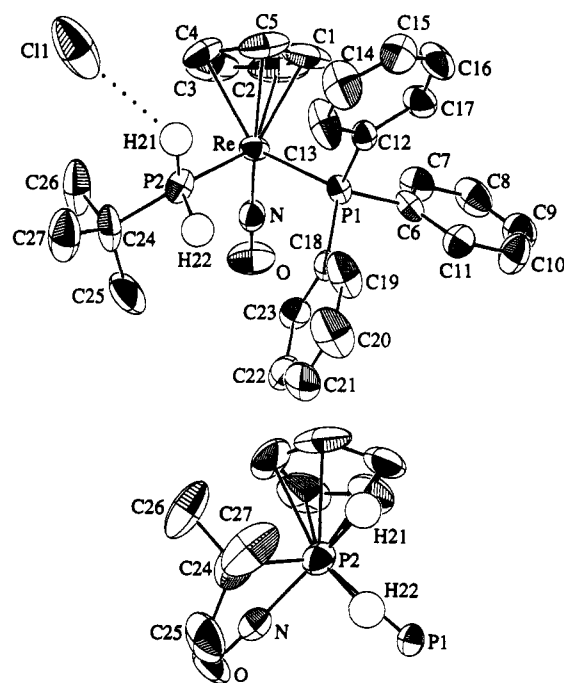


**Figure 3.** Structure of *tert*-butylphosphine complex  $2\text{c}^+\text{Cl}^- \cdot 0.5\text{CH}_2\text{Cl}_2$ : top, numbering diagram; bottom, Newman-type projection of the cation down the P2-Re bond with the  $\text{PPh}_3$  phenyl groups omitted.

Experimental Section, yielded the structure shown in Figure 3. Both phosphorus-bound hydrogen atoms were located ( $\text{H}_S/\text{H}_R = \text{H}21/\text{H}22$ ). Atomic coordinates, and key bond lengths, bond angles, and torsion angles, are listed in Tables IV and V. A table of anisotropic thermal parameters is given in the supplementary material.

Although the metrical parameters associated with the PH protons have considerable experimental error, they

(21) Studies of  $\text{P}\cdots\text{H}\cdots\text{X}$  hydrogen bonding in solution (X = I, Br, Cl, F): van den Akker, M.; Jellinek, F. *Recl. Trav. Chim. Pays-Bas* 1967, 86, 275.

Table IV. Atomic Coordinates and Equivalent Isotropic Thermal Parameters of Located Atoms in  $2c^+Cl^- \cdot 0.5CH_2Cl_2$  and  $(RS,SR)\text{-}5^+TfO^-$ 

atom	x	y	z	B, Å <sup>2</sup>	atom	x	y	z	B, Å <sup>2</sup>
$2c^+Cl^- \cdot 0.5CH_2Cl_2$					$(RS,SR)\text{-}5^+TfO^-$				
Re	0.15988 (2)	0.07594 (2)	0.06819 (2)	2.821 (6)	Re	0.10989 (3)	0.16153 (4)	0.11873 (1)	3.959 (7)
Cl1	0.2212 (3)	-0.0336 (2)	0.3039 (3)	11.0 (1)	P1	0.2985 (2)	0.0568 (3)	0.11686 (8)	3.99 (5)
Cl2	0.5217 (3)	0.0723 (3)	0.0187 (3)	10.1 (1)	P2	0.1938 (3)	0.3475 (3)	0.16853 (8)	4.97 (6)
P1	0.1881 (2)	0.2003 (1)	0.0603 (1)	2.55 (5)	O	0.0524 (7)	-0.0505 (9)	0.1837 (2)	7.7 (2)
P2	0.0997 (2)	0.0891 (1)	0.1773 (1)	3.51 (6)	N	0.0788 (7)	0.0373 (9)	0.1592 (2)	4.7 (2)
O	-0.0048 (5)	0.0856 (5)	-0.0089 (4)	5.4 (2)	C1	0.075 (1)	0.164 (1)	0.0413 (3)	5.5 (2)
N	0.0596 (5)	0.0836 (4)	0.0238 (4)	3.2 (2)	C2	-0.020 (1)	0.087 (1)	0.0569 (4)	7.2 (3)
C1	0.2941 (8)	0.0512 (7)	0.0271 (8)	6.7 (4)	C3	-0.080 (1)	0.185 (1)	0.0819 (4)	6.7 (3)
C2	0.2409 (9)	0.0039 (8)	-0.0016 (8)	7.6 (3)	C4	-0.026 (1)	0.317 (1)	0.0813 (4)	7.3 (3)
C3	0.2067 (8)	-0.0338 (6)	0.052 (1)	8.2 (5)	C5	0.072 (1)	0.308 (1)	0.0567 (3)	6.7 (3)
C4	0.243 (1)	-0.0136 (7)	0.1151 (7)	6.7 (3)	C6	0.2982 (8)	-0.070 (1)	0.0711 (3)	4.2 (2)
C5	0.2990 (8)	0.0422 (7)	0.0950 (7)	5.8 (3)	C7	0.3868 (9)	-0.076 (1)	0.0458 (3)	5.5 (3)
C6	0.1935 (6)	0.2339 (5)	-0.0265 (5)	3.0 (2)	C8	0.385 (1)	-0.182 (1)	0.0135 (4)	7.1 (3)
C7	0.1987 (7)	0.1883 (6)	-0.0816 (5)	3.9 (2)	C9	0.297 (1)	-0.284 (1)	0.0065 (4)	6.7 (3)
C8	0.2049 (8)	0.2175 (7)	-0.1468 (5)	5.0 (3)	C10	0.208 (1)	-0.281 (1)	0.318 (4)	5.8 (3)
C9	0.2038 (8)	0.2898 (7)	-0.1547 (6)	5.3 (3)	C11	0.2066 (9)	-0.175 (1)	0.0640 (3)	4.8 (2)
C10	0.1997 (9)	0.3359 (6)	-0.1017 (6)	4.8 (3)	C12	0.4181 (9)	0.180 (1)	0.1121 (3)	6.1 (2)
C11	0.1941 (7)	0.3083 (6)	-0.0372 (5)	3.7 (2)	C13	0.400 (1)	0.287 (1)	0.0808 (5)	9.0 (3)
C12	0.2915 (6)	0.2250 (5)	0.0990 (5)	2.8 (2)	C14	0.488 (1)	0.386 (2)	0.0759 (6)	12.2 (5)
C13	0.3007 (8)	0.2205 (8)	0.1687 (5)	5.6 (3)	C15	0.590 (1)	0.376 (2)	0.1034 (5)	12.2 (4)
C14	0.3766 (9)	0.2401 (8)	0.2004 (6)	6.2 (3)	C16	0.618 (1)	0.266 (2)	0.1365 (5)	12.1 (5)
C15	0.4473 (8)	0.2631 (7)	0.1643 (6)	5.0 (3)	C17	0.529 (1)	0.168 (2)	0.1406 (4)	8.2 (3)
C16	0.4418 (7)	0.2636 (7)	0.0947 (6)	5.1 (3)	C18	0.3592 (8)	-0.054 (1)	0.1654 (3)	4.6 (2)
C17	0.3650 (7)	0.2456 (6)	0.0633 (6)	4.3 (2)	C19	0.430 (1)	-0.172 (2)	0.1608 (4)	6.7 (3)
C18	0.1065 (6)	0.2599 (5)	0.0985 (5)	2.8 (2)	C20	0.479 (1)	-0.257 (2)	0.1978 (5)	8.4 (4)
C19	0.1323 (8)	0.3178 (6)	0.1379 (6)	5.8 (3)	C21	0.455 (1)	-0.221 (2)	0.2393 (4)	7.7 (3)
C20	0.069 (1)	0.3604 (7)	0.1663 (7)	7.6 (4)	C22	0.384 (1)	-0.107 (1)	0.2443 (4)	6.6 (3)
C21	-0.0200 (9)	0.3467 (6)	0.1552 (6)	6.1 (3)	C23	0.3371 (9)	-0.025 (1)	0.2072 (3)	5.3 (2)
C22	-0.0459 (8)	0.2901 (6)	0.1159 (6)	4.7 (3)	C24	0.122 (1)	0.391 (1)	0.2172 (3)	6.0 (3)
C23	0.0188 (7)	0.2454 (5)	0.0883 (5)	3.5 (2)	C25	0.139 (1)	0.263 (2)	0.2490 (3)	7.9 (4)
C24	-0.0046 (9)	0.0433 (6)	0.1968 (6)	5.2 (3)	C26	-0.009 (1)	0.416 (2)	0.2009 (4)	9.6 (4)
C25	-0.0801 (7)	0.0797 (9)	0.1594 (7)	6.9 (4)	C27	0.176 (1)	0.524 (2)	0.2413 (4)	9.7 (4)
C26	0.003 (1)	-0.0353 (6)	0.1785 (7)	6.7 (3)	C28	0.210 (1)	0.519 (1)	0.1399 (4)	7.5 (3)
C27	-0.018 (1)	0.0495 (7)	0.2743 (7)	7.5 (4)	C29	0.256 (2)	0.292 (2)	0.3964 (6)	10.9 (6)
C28	0.488 (2)	0.492 (1)	0.448 (1)	13.8 (8)	F1	0.729 (1)	0.892 (1)	0.1283 (3)	13.0 (3)
H21*	0.168	0.082	0.215	5.0	F2	0.6325 (7)	0.766 (1)	0.1007 (4)	15.0 (4)
H22*	0.084	0.166	0.215	5.0	F3	0.763 (2)	0.686 (3)	0.1422 (5)	22.1 (8)
					O1	0.9369 (8)	0.737 (1)	0.0772 (5)	15.0 (4)
					O2	0.756 (1)	0.602 (1)	0.0443 (4)	16.4 (4)
					O3	0.219 (2)	0.328 (2)	0.4646 (5)	23.1 (8)
					S	0.8217 (3)	0.6991 (4)	0.0706 (1)	7.54 (8)
					H22	0.321 (9)	0.33 (1)	0.184 (3)	5.0

\* Atoms refined anisotropically are given in the form of the isotropic equivalent displacement parameter, defined as  $(4/3)[a^2B(1,1) + b^2B(2,2) + c^2B(3,3) + ab(\cos \gamma)B(1,2) + ac(\cos \beta)B(1,3) + bc(\cos \alpha)B(2,3)]$ . The starred atoms were located but their positions were not refined.

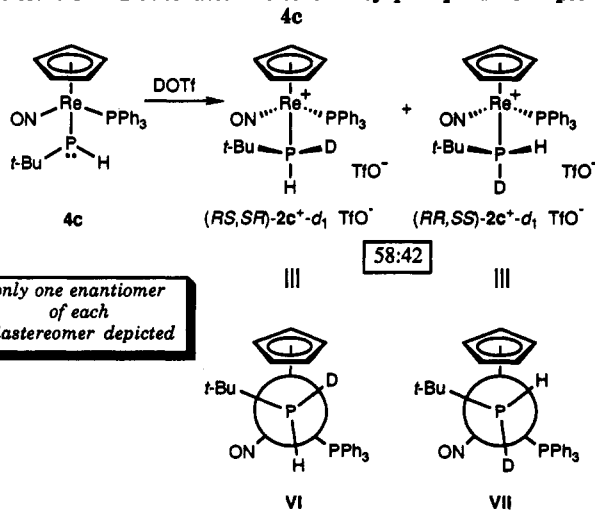
provide support for a  $P \cdots H_S \cdots Cl$  hydrogen bond in crystalline  $2c^+Cl^- \cdot (CH_2Cl_2)_{0.5}$ . Most importantly, the  $H_S \cdots Cl$  contact (2.90 Å) is less than the sum of the van der Waals radii (2.95–3.00 Å)<sup>22,23</sup> and similar to that in other  $P \cdots H \cdots X$  interactions.<sup>24</sup> The distance between  $H_R$  and Cl is much greater (4.63 Å), and the P/Cl termini of the hydrogen bond are separated by only 3.87 Å. Another noteworthy feature is the  $Re-PRH_2$  conformation, which is analogous to that established for  $2c^+TfO^-$  in solution. The  $Ph_3P-Re-P-H$  torsion angles ( $5^\circ$ ,  $H_R$ ;  $-89^\circ$ ,  $H_S$ ) are in good agreement with those expected from the  $^3J_{HP}$  data and the Karplus relationship.

The hydrogen bond in  $2c^+Cl^-$  constitutes a potential transition-state model for deprotonation to the phosphido complex **4c**. In this event, only one of the two diastereotopic PH protons in  $2c^+X^-$  would be abstracted by base.

(22) Moeller, T. *Inorganic Chemistry*; Wiley: New York, 1982; pp 67–73.

(23) Whuler, A.; Brouty, C.; Spinat, P. *Acta Crystallogr.* 1980, B36, 1267. Much structural data are available for  $N \cdots H \cdots Cl$  hydrogen bonds in complexes of the type  $[L_2M(NRH_2)]^+nCl^-$ . The  $H \cdots Cl$  distances range from 2.4 to 2.9 Å.

(24)  $P \cdots H \cdots I$  in  $PH_4^+I^-$  (2.87 Å;  $\angle 171.6^\circ$ ): Sequeira, A.; Hamilton, W. C. *J. Chem. Phys.* 1967, 47, 1818.

Scheme IV. Deuteration of *tert*-Butylphosphido Complex

Deuterated derivatives were sought that would enable this possibility to be tested. Thus, a  $-80^\circ C$  THF solution of **4c** was slowly added to a  $-80^\circ C$  THF solution of triflic acid- $d_1$  (1.2 equiv). Workup gave  $2c^+-d_1 TfO^-$  that was only

Table V. Selected Bond Lengths (Å), Bond Angles (deg), and Torsion Angles (deg) in  $2c^+Cl^- \cdot 0.5CH_2Cl_2$  and  $(RS,SR)\text{-}5^+TfO^-$ <sup>a</sup>

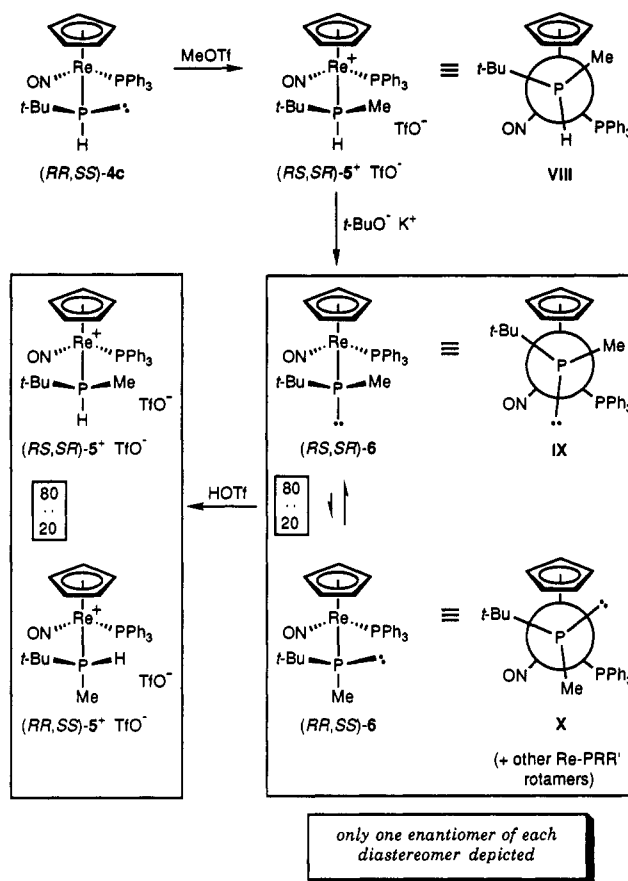
	$2c^+Cl^-(CH_2Cl_2)_{0.5}$	$(RS,SR)\text{-}5^+TfO^-$
Re-P1	2.370 (2)	2.384 (1)
Re-P2	2.361 (2)	2.373 (2)
Re-N	1.772 (6)	1.765 (4)
N-O	1.177 (7)	1.177 (5)
P1-C6	1.831 (7)	1.818 (5)
P1-C12	1.814 (6)	1.811 (6)
P1-C18	1.834 (6)	1.828 (5)
P2-H21	1.29	
P2-H22	1.64	1.46 (6)
H21-C11	2.90	
P2-C24	1.847 (8)	1.868 (6)
C24-C25	1.53 (1)	1.518 (9)
C24-C26	1.52 (1)	1.51 (1)
C24-C27	1.55 (1)	1.505 (9)
Re-C1	2.252 (8)	2.316 (5)
Re-C2	2.291 (9)	2.282 (6)
Re-C3	2.285 (8)	2.271 (7)
Re-C4	2.297 (8)	2.264 (6)
Re-C5	2.278 (8)	2.293 (6)
C1-C2	1.33 (1)	1.453 (9)
C1-C5	1.36 (1)	1.412 (9)
C2-C3	1.43 (2)	1.44 (1)
C3-C4	1.45 (2)	1.36 (1)
C4-C5	1.40 (1)	1.46 (1)
P1-Re-P2	91.66 (6)	92.45 (5)
P1-Re-N	92.6 (2)	93.1 (1)
P2-Re-N	96.3 (2)	97.8 (1)
Re-N-O	175.5 (5)	175.0 (4)
Re-P1-C6	114.0 (2)	113.9 (2)
Re-P1-C12	112.3 (2)	117.0 (2)
Re-P1-C18	116.5 (2)	115.0 (2)
C2-C1-C5	112.0 (1)	106.6 (6)
C1-C2-C3	106.0 (1)	108.9 (6)
C2-C3-C4	108.6 (9)	107.0 (6)
C3-C4-C5	103.3 (9)	110.5 (7)
C1-C5-C4	109.9 (9)	106.9 (6)
Re-P2-C24	118.6 (3)	118.2 (2)
P2-C24-C25	110.1 (5)	108.0 (4)
P2-C24-C26	109.2 (6)	109.4 (4)
P2-C24-C27	106.5 (6)	110.6 (5)
Re-P2-H22	124	115 (2)
Re-P2-C28		112.7 (2)
Re-P2-H21	102	
C24-P2-H22	114	109 (2)
C24-P2-C28		106.7 (3)
H22-P2-C28		93 (2)
H22-P2-H21	87	
P2-H21-C11	131	
P1-Re-P2-C24	134.1 (5)	135.2 (4)
P1-Re-P2-H22	5	5 (4)
P1-Re-P2-H21	-89	
P1-Re-P2-C28		-99.5 (5)
N-Re-P2-C24	41.3 (5)	41.7 (5)
N-Re-P2-H22	-88	-89 (4)
N-Re-P2-H21	178	
N-Re-P2-C28		167.0 (6)

<sup>a</sup> Since hydrogen atom positions were not refined in  $2c^+Cl^- \cdot 0.5CH_2Cl_2$ , estimated standard deviations are not given for the corresponding metrical parameters.

a ( $58 \pm 2$ ):( $42 \pm 2$ ) mixture of *RS,SR/RR,SS* diastereomers (Scheme IV), as assayed by <sup>1</sup>H NMR spectroscopy. An opposite order of acid addition gave lower diastereoselectivity, and identical results were obtained in NMR monitored reactions. In view of the modest label fidelity, deprotonation studies were not pursued.

**6. Diastereoselective Alkylation of 4c.** Finally, we sought to study reactions of **4** and alkylating agents. Hence, a benzene solution of **4c** was treated with methyl triflate (1.5 equiv). A simple precipitation gave the secondary phosphine complex  $[(\eta^5\text{-C}_5\text{H}_5)\text{Re}(\text{NO})(\text{PPh}_3)(\text{P}(t\text{-Bu})\text{MeH})]^+\text{TfO}^-$  (**5**<sup>+</sup>TfO<sup>-</sup>) as a powder in 95% yield

Scheme V. Diastereoselective Methylation of *tert*-Butylphosphido Complex **4c**



(Scheme V). An analytical sample was prepared and characterized similarly to the other new compounds described above. By all criteria, the crude and purified product was a single diastereomer (>98% de).

In order to unequivocally assign structure, X-ray data were collected on **5**<sup>+</sup>TfO<sup>-</sup> as summarized in Table III. Refinement gave the structure shown in Figure 4—a *RS,SR* diastereomer. The PH proton (H22) was located. Atomic coordinates, and key bond lengths, bond angles, and torsion angles, are listed in Tables IV and V. A table of anisotropic thermal parameters is given in the supplementary material.

The triflate anion in  $(RS,SR)\text{-}5^+TfO^-$  showed some degree of thermal disorder. Nonetheless, distances between the triflate oxygens and H22 were bounded as 6.2–6.9 Å, thus showing hydrogen bonding to be absent. Also,  $(RS,SR)\text{-}5^+TfO^-$  was subjected to a difference <sup>1</sup>H NOE experiment. Irradiation of the cyclopentadienyl resonance (87%) gave enhancements of 3.1% in the methyl protons, 1.0% in the *tert*-butyl protons, and 2.9% in the ortho PPh<sub>3</sub> ligand protons. These data indicate that the Re-PHRR' rotamer found in the solid state also dominates in solution.

Next,  $(RS,SR)\text{-}5^+TfO^-$  was treated with *t*-BuO<sup>-</sup>K<sup>+</sup> (Scheme V). Workup gave the *tert*-butylmethylphosphido complex  $(\eta^5\text{-C}_5\text{H}_5)\text{Re}(\text{NO})(\text{PPh}_3)(\text{P}(t\text{-Bu})\text{Me})$  (**6**) in 85% yield. Complex **6** was much more air sensitive than **4a-c**. When <sup>1</sup>H or <sup>31</sup>P NMR spectra were recorded in THF-*d*<sub>6</sub> at -25 °C, a ( $80 \pm 2$ ):( $20 \pm 2$ ) mixture of diastereomers was observed. Their resonances coalesced upon warming, and selected data are given in Table II.<sup>25</sup> The  $\Delta G^\ddagger_{T(c)}$  values were slightly greater than those of the primary phosphido complexes **4a,b**.

(25) Variable-temperature NMR spectra are depicted in ref 8b.



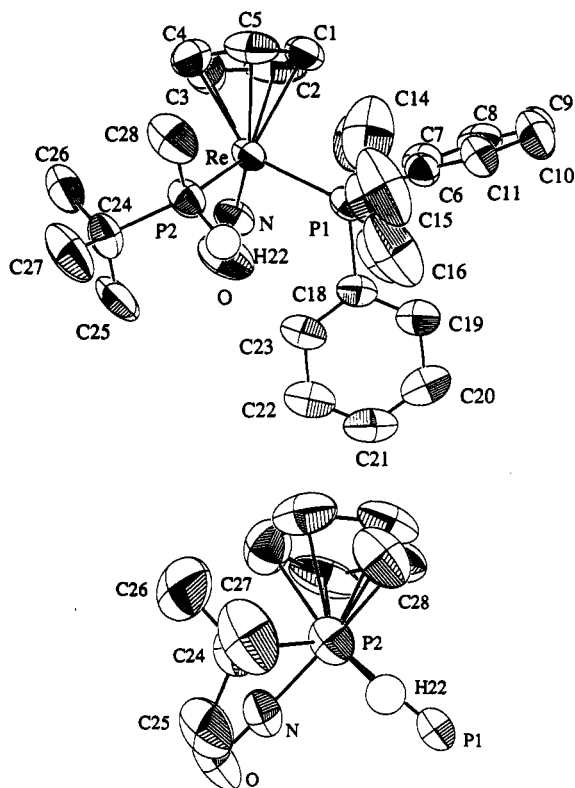
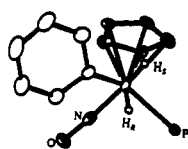


**Figure 4.** Structure of the cation of secondary phosphine complex  $(RS,SR)-5^+TfO^-$ : top, numbering diagram; bottom, Newman-type projection down the P2-Re bond with the PPh<sub>3</sub> phenyl groups omitted.

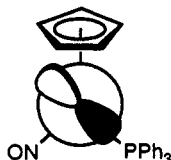
A benzene solution of **6** was treated with triflic acid (Scheme V). Workup gave a  $(80 \pm 2):(20 \pm 2)$  mixture of  $(RS,SR)-5^+TfO^-$  and a new diastereomer,  $(RR,SS)-5^+TfO^-$  (93%). Complete NMR data for both compounds are given in Table I. The transition state for protonation almost certainly involves retention of configuration at phosphorus—i.e., “frontside” attack upon the lone pair. Thus, only  $(RS,SR)-6$  can give  $(RS,SR)-5^+TfO^-$ , and only  $(RR,SS)-6$  can give  $(RR,SS)-5^+TfO^-$ . Since the diastereomer ratios of the reactants and products in Scheme V exactly match,  $(RS,SR)-6$  can be confidently assigned as the more stable phosphido complex diastereomer.

### Discussion

**1. Structures of Phosphine Complexes.** Several prior structural studies of related compounds are relevant to our data with the primary phosphine complexes  $2^+X^-$ . For example, the benzyl complex  $(\eta^5-C_5H_5)Re(NO)(PPh_3)(CH_2Ph)$  (**7**) adopts a solid-state  $Re-CH_2Ph$  conformation that places the phenyl substituent in the spacious interstice between the nitrosyl and cyclopentadienyl ligands (see XI),<sup>14a</sup> similar to the *tert*-butyl substituent position in  $2c^+Cl^-0.5CH_2Cl_2$  (Figure 3). However, the



XI



XII

$$\begin{aligned} \angle P-Re-C-C &= 157^\circ & \angle N-Re-C-C &= 63^\circ \\ \angle P-Re-C-H_R &= 39^\circ & \angle N-Re-C-H_R &= -54^\circ \\ \angle P-Re-C-H_S &= -94^\circ & \angle N-Re-C-H_S &= 173^\circ \end{aligned}$$

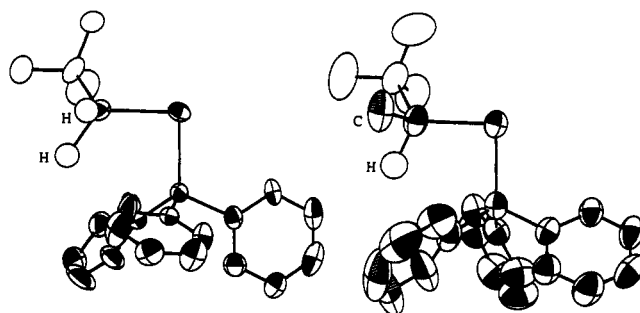


**Figure 5.** Views of the PPh<sub>3</sub> rotors of  $2c^+Cl^-0.5CH_2Cl_2$  (left) and  $(RS,SR)-5^+TfO^-$  (right).

ON-Re-X-C torsion angle in **7** is somewhat greater ( $63^\circ$  vs  $41^\circ$ ). Thus, the bulkier *tert*-butyl substituent is displaced further from the medium-sized cyclopentadienyl ligand and toward the small nitrosyl ligand.

Monodeuterated derivatives of **7** and the analogous ethyl complex have been prepared with labels exclusively in the H<sub>R</sub> and H<sub>S</sub> positions.<sup>26</sup> In contrast to  $2^+X^-$ , the H<sub>S</sub> <sup>1</sup>H NMR resonances are *upfield* of the H<sub>R</sub> resonances. However, in accord with the Karplus relationship<sup>15-17</sup> and agreement with  $2^+X^-$ , H<sub>R</sub> exhibits the larger <sup>3</sup>J<sub>HP</sub> values (7, 8.0 vs 3.0 Hz).<sup>27</sup> Also, <sup>1</sup>H NOE experiments with other alkyl complexes  $(\eta^5-C_5H_5)Re(NO)(PPh_3)(CH_2R)$  show ca. 1% enhancements of the H<sub>S</sub> resonances upon cyclopentadienyl ligand irradiation but none for H<sub>R</sub>.<sup>28</sup> Interestingly, the <sup>3</sup>J<sub>HP</sub> value for H<sub>R</sub> in  $2c^+TfO^-$  is ca. 2 Hz greater than those of **2a,b**<sup>+</sup>X<sup>-</sup> (Table I). This suggests a greater displacement of the *tert*-butyl group from the cyclopentadienyl ligand, as analyzed for  $2c^+TfO^-$  and **7**, with a consequential decrease in the Ph<sub>3</sub>P-Re-P-H<sub>R</sub> torsion angle to a value closer to  $0^\circ$ .

The crystal structures of the primary phosphine complex  $2c^+Cl^-0.5CH_2Cl_2$  and the secondary phosphine complex  $(RS,SR)-5^+TfO^-$  (Figures 3 and 4) exhibit considerable homology with regard to bond lengths and angles about rhenium (Table V). Also, the torsion angles about the Re-PRR/H bonds are virtually identical. The absence of any perturbation by the methyl group in  $(RS,SR)-5^+TfO^-$  suggests that the *tert*-butyl groups are the principal determinants of Re-PRR/H conformation.

The four Re-P bonds in  $2c^+Cl^-0.5CH_2Cl_2$  and  $(RS,SR)-5^+TfO^-$  (2.361 (2)–2.384 (1) Å) are much shorter than the Re-PR<sub>2</sub> bonds in symmetrically-substituted phosphido complexes  $(\eta^5-C_5H_5)Re(NO)(PPh_3)(PR_2)$  (R = Ph, *t*-Bu; 2.461 (3)–2.526 (4) Å).<sup>4</sup> This can be chiefly ascribed to the removal of repulsive interactions between the phosphido phosphorus lone pair and filled metal orbitals—such as the d orbital HOMO shown in XII<sup>29</sup>—as analyzed earlier.<sup>4b</sup> The Re-PPh<sub>3</sub> bond lengths (2.370 (2)–2.384 (1) Å) are essentially identical with those in  $(\eta^5-C_5H_5)Re(NO)-(PPh_3)(PR_2)$  (2.358 (3)–2.357 (4) Å).

Crystalline  $2c^+Cl^-0.5CH_2Cl_2$  and  $(RS,SR)-5^+TfO^-$  differ in one very interesting aspect. Namely, the PPh<sub>3</sub> ligands, which constitute stereocenters due to their propeller-like geometries,<sup>30</sup> adopt opposite helical pitches. This feature

(26) (a) Kiel, W. A.; Lin, G.-Y.; Constable, A. G.; McCormick, F. B.; Strouse, C. E.; Eisenstein, O.; Gladysz, J. A. *J. Am. Chem. Soc.* 1982, 104, 4865. (b) Kiel, W. A.; Lin, G.-Y.; Bodner, G. S.; Gladysz, J. A. *Ibid.* 1983, 105, 4958.

(27) The iron alkyl complex  $(\eta^5-C_5H_5)Fe(CO)(PPh_3)(CH_2SiMe_3)$  also bears an obvious steric relationship to  $2c^+X^-$ .<sup>16a</sup> It exhibits Ph<sub>3</sub>P-Fe-C-X torsion angles of  $147^\circ$ ,  $24^\circ$ , and  $-87^\circ$  (X = Si, H<sub>R</sub>, H<sub>S</sub>). The H<sub>R</sub> <sup>1</sup>H NMR resonance is upfield from that of H<sub>S</sub>, and exhibits a larger <sup>3</sup>J<sub>HP</sub> value (13.8 vs 1.9 Hz).

(28) Bodner, G. S.; Emerson, K.; Larsen, R. D.; Gladysz, J. A. *Organometallics* 1989, 8, 2399.

is illustrated in the partial structures in Figure 5. In solution, the rotor configurations rapidly invert ( $\Delta G^\ddagger \leq 5$  kcal/mol),<sup>30c</sup> and distinct diastereomers are not detected. In the solid state, lattice forces might influence the configuration. However, if these are negligible in Figures 3–5, then the replacement of  $H_S \cdot Cl$  in  $2c^+Cl \cdot 0.5CH_2Cl_2$  by the larger methyl group in  $(RS,SR)-5^+TfO^-$  is responsible for inverting the screw sense of the  $PPh_3$  rotor. In other chiral-at-metal complexes, the configurations of phosphine rotors have been viewed primarily as a function of metal chirality.<sup>30c</sup>

**2. Hydrogen Bonding.** Over the past few years, a variety of metal complexes of the general formula  $L_nMXR_n$  have been shown to form hydrogen bonds—often to acids as weak as phenols.<sup>31–34</sup> We have demonstrated that the nitrogen lone pairs in amido complexes  $(\eta^5-C_5H_5)Re(NO)(PPh_3)(\dot{N}RR')$  are much more basic and nucleophilic than those in organic amines and suspect that similar trends hold for most coordinatively saturated  $L_nMXR_n$  complexes.<sup>10c</sup> Thus, the donor atoms in such molecules should generally be superior hydrogen bond acceptors. Conversely, the conjugate acids  $[L_nMXHR_n]^+$  (such as cations  $2^+$ ) should be somewhat less effective hydrogen bond donors than organic analogues.

Surprisingly, there appear to be relatively few studies of  $P \cdot H \cdot X$  hydrogen bonds in the literature.<sup>21,24</sup> Our data show that, in solution, the chloride ion more readily bonds to  $2c^+$  than the triflate ion. This trend is consistent with the Brønsted acidity order  $TfOH > HCl$ .<sup>35</sup> Thus, the chloride ion is the stronger conjugate base. Also, chloride ion deprotonates cationic metal hydride complexes more rapidly than the more basic acetate ion.<sup>36</sup>

Although our data also provide good evidence for hydrogen bonding in crystalline  $2c^+Cl \cdot (CH_2Cl_2)_{0.5}$ , such phenomena can be capriciously influenced by packing forces. For example, the dimethylamine complex  $[(\eta^5-C_5H_5)Re(NO)(PPh_3)(NHMe_2)]^+TfO^-$  crystallizes with a  $N \cdot H \cdot OTf$  hydrogen bond, although there is no evidence for any interaction in solution.<sup>9b</sup> Similarly, some ruthenium amine complexes of the formula  $[(\eta^5-C_5H_5)Ru(L)_2(NHRR')]^+TfO^-$  crystallize with  $N \cdot H \cdot OTf$  hydrogen bonds, whereas others do not.<sup>34</sup>

Finally, the diastereoselective nature of the hydrogen bonding in  $2c^+Cl^-$  suggests that the  $H_S$  protons are kinetically more acidic than the  $H_R$  protons. However, the

PH proton of the secondary phosphine complex  $(RS,SR)-5^+TfO^-$ , which occupies a position analogous to that of  $H_R$  in  $2^+X^-$ , is also readily abstracted by  $t-BuO^-K^+$ . Thus, both types of protons are in principle accessible to base, and rigorous experimental tests must await routes to deuterated derivatives that are more diastereoselective than that in Scheme IV.<sup>37</sup>

**3. Structures of Phosphido Complexes.** Theoretical studies of the model compound  $(\eta^5-C_5H_5)Re(NO)(PH_3)(\dot{P}H_2)$  revealed only two minima—corresponding to II and III in Scheme II—as the  $Re-\dot{P}H_2$  bond was rotated through  $360^\circ$ .<sup>4b</sup> As has been previously discussed in detail, these conformations lessen overlap of the phosphido ligand lone pair with the rhenium fragment d orbital HOMO (XII), while avoiding eclipsing interactions. In the solid state, symmetrically-substituted secondary phosphido complexes  $(\eta^5-C_5H_5)Re(NO)(PPh_3)(\dot{P}R_2)$  exhibit  $Re-\dot{P}R_2$  conformations analogous to that in III.<sup>4</sup>

As noted above, II and III can be confidently represented as the most stable  $Re-\dot{P}RH$  rotamers of the  $RR,SS$  and  $RS,SR$  diastereomers of 4. Any alternative places the alkyl group in a more congested interstice. However, diastereomer assignments are less straightforward. A potential clue is provided by the diastereoselective methylation of 4c to  $(RS,SR)-5^+TfO^-$  (Scheme V). The product (VIII) can form only from the  $RR,SS$  diastereomer of 4c (II). Together with the deuteration results in Scheme IV, it is clear that  $(RR,SS)-4c$  is more reactive toward electrophiles than  $(RS,SR)-4c$ .

The secondary phosphido complexes  $(RS,SR)-6$  and  $(RR,SS)-6$ , for which configurations and relative stabilities can be assigned from the reactions in Scheme V, provide the Rosetta stone that unravels these assignments. As summarized in Table I, the  $PPh_3$   $^{31}P$  NMR resonance of the less stable  $RR,SS$  diastereomer (24.07 ppm) is downfield of that of the more stable  $RS,SR$  diastereomer (16.07 ppm) and exhibits a much smaller  $^2J_{PP}$  value (<2 vs 30 Hz). The *tert*-butylphosphido complex 4c, which appears to be diastereomerically homogeneous, exhibits a very similar chemical shift (25.80 ppm) and  $^2J_{PP}$  value (<3 Hz), suggestive of an  $RR,SS$  diastereomer and in accord with the reactivity data.

More importantly,  $^{31}P$  NMR data are available for both diastereomers of the methylphosphido complex 4b. The more stable diastereomer exhibits a chemical shift (25.65 ppm) and  $^2J_{PP}$  value (6.5 Hz) similar to those of  $(RR,SS)-6$  and 4c, while the less stable diastereomer gives chemical shift and  $^2J_{PP}$  values (21.28 ppm, 19.1 Hz) closer to those of  $(RS,SR)-6$ . The diastereomers of phenylphosphido complex 4a exhibit analogous  $^{31}P$  NMR patterns (24.22 vs 18.72 ppm; <2 vs 15.4 Hz). Hence, we assign the diastereomers of 4 with the downfield  $PPh_3$   $^{31}P$  NMR resonances and smaller  $^2J_{PP}$  values  $RR,SS$  configurations (II).<sup>38</sup>

Significantly, logical corollaries of these assignments rationalize the trends in  $RR,SS/RS,SR$  equilibrium ratios ( $4c > 4b > 4a > 6$ ). First, the large *tert*-butyl substituent in 4c should effect the greatest counterclockwise distortions from the idealized  $Re-\dot{P}RH$  conformations shown in

(29) (a) Schilling, B. E. R.; Hoffmann, R.; Faller, J. *J. Am. Chem. Soc.* 1979, 101, 592. (b) Georgiou, S.; Gladysz, J. A. *Tetrahedron* 1986, 42, 1109. (c) Czech, P. T.; Gladysz, J. A.; Fenske, R. F. *Organometallics* 1989, 8, 1806.

(30) (a) Bye, E.; Schweizer, W. B.; Dunitz, J. D. *J. Am. Chem. Soc.* 1982, 104, 5893. (b) Brunner, H.; Hammer, B.; Krüger, C.; Angermund, K.; Bernal, I. *Organometallics* 1985, 4, 1063. (c) Davies, S. G.; Derome, A. E.; McNalley, J. P. *J. Am. Chem. Soc.* 1991, 113, 2854.

(31) (a) Kegley, S. E.; Schaverien, C. J.; Freudenberger, J. H.; Bergman, R. G.; Nolan, S. P.; Hoff, C. D. *J. Am. Chem. Soc.* 1987, 109, 6563. (b) Klein, D. P.; Hayes, J. C.; Bergman, R. G. *J. Am. Chem. Soc.* 1988, 110, 3704.

(32) (a) Richmond, T. G. *Coord. Chem. Rev.* 1990, 105, 221. (b) Di Bugno, C.; Pasquali, M.; Leoni, P.; Sabatino, P.; Braga, D. *Inorg. Chem.* 1989, 28, 1390.

(33) (a) Kim, Y.-J.; Osakada, K.; Takenaka, A.; Yamamoto, A. *J. Am. Chem. Soc.* 1990, 112, 1096. (b) Osakada, K.; Kim, Y.-J.; Yamamoto, A. *J. Organomet. Chem.* 1990, 382, 303. (c) Osakada, K.; Ohshiro, K.; Yamamoto, A. *Organometallics* 1991, 10, 404. (d) Osakada, K.; Kim, Y.-J.; Tanaka, M.; Ishiguro, S.; Yamamoto, A. *Inorg. Chem.* 1991, 30, 197.

(34) Joslin, F. L.; Johnson, M. P.; Mague, J. T.; Roundhill, D. M. *Organometallics* 1991, 10, 2781. Relevant hydrogen atom positions are given in the supplementary material of this paper.

(35) (a) McCallum, C.; Pethybridge, A. D. *Electrochim. Acta* 1975, 20, 815. (b) Cox, R. A.; Krull, U. J.; Thompson, M.; Yates, K. *Anal. Chim. Acta* 1979, 106, 51.

(36) (a) Darensbourg, M. Y.; Hanckel, J. M. *J. Am. Chem. Soc.* 1983, 105, 6979. (b) Darensbourg, M. Y.; Ludvig, M. M. *Inorg. Chem.* 1986, 25, 2894.

(37) We are not certain that the data in Scheme IV reflect an intrinsically nonselective deuteration, as opposed to some secondary scrambling process. Some very puzzling results involving interconversion of deuterated  $2b^+TfO^-$  and 4b have been obtained.<sup>36</sup>

(38) Other NMR trends involving 4a–c and 6 are evident. For example, the  $PRR'$   $^{31}P$  NMR resonances of  $(RR,SS)-4,6$  are downfield of those of  $(RS,SR)-4,6$  and give the smaller  $^2J_{PP}$  values. Also,  $(RR,SS)-4b,c$  exhibit PH  $^1H$  NMR resonances at  $\delta$  3.28 and 3.53 with  $^3J_{HP}$  values of 8.0 and 10.6 Hz. The diastereomers of 4a exhibit PH  $^1H$  NMR resonances at  $\delta$  3.74 and 3.34 with  $^3J_{HP}$  values of ca. 10 and <2 Hz. These are assigned to  $(RR,SS)-4a$  and  $(RS,SR)-4a$ , respectively, as verified by the  $^1J_{PH}$  values in Table I (see footnote g).

II and III. This will diminish overlap of the  $\dot{P}RH$  lone pair with the rhenium fragment HOMO in II, providing stabilization, but enhance overlap in III, effecting destabilization.

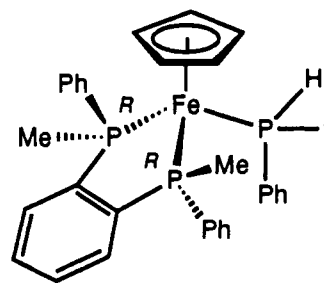
Any torsional distortion in 4b, which has a smaller methyl substituent, should be lower. Accordingly, the equilibrium is less biased. The unsaturated phenyl substituent in 4a can potentially exert an electronic effect upon the equilibrium. However, by some steric criteria a phenyl ring is smaller than a methyl group.<sup>39</sup> Finally, the interstice between the bulky  $PPh_3$  ligand and nitrosyl ligand is the sterically most congested.<sup>16</sup> Thus, the replacement of the PH hydrogen in II by a larger alkyl group can give severe destabilizing interactions. This effect, and possibly secondary torsional consequences, accounts for the inversion of  $RR,SS/RS,SR$  diastereomer stabilities with 6.

The phosphido complex diastereomer ratios can be viewed as a measure of chiral recognition—i.e., the relative ease of fit of two configurations of a labile  $\dot{P}RR'$  stereocenter to one configuration of the  $[(\eta^5-C_5H_5)Re(NO)-(PPh_3)]^+$  fragment. Interestingly, the phenylamido complex  $(\eta^5-C_5H_5)Re(NO)(PPh_3)(NPh)$  (8), which is isosteric with 4a, crystallizes as an  $RS,SR$  diastereomer, with a  $Re-NPh$  conformation analogous to the  $Re-\dot{P}RH$  conformation in III.<sup>10b,c</sup> The diastereomers of 8 and related species interconvert much more rapidly than those of 4. Hence, solution equilibrium data are not available.

**4. Dynamic and Chemical Properties of Phosphido Complexes.** In essence, the diastereomers of 4 can equilibrate by a simple bending motion of the phosphorus-hydrogen bond. This is illustrated by the transition state IV in Scheme II. Only a slight additional torsional motion about the  $Re-\dot{P}RH$  bond is required along the reaction coordinate. Thus, the  $\Delta G^\ddagger_{T(c)}$  values for diastereomer interconversion (Table II) must very closely approximate the phosphorus inversion barriers. Interestingly, that measured for the phenylphosphido complex 4a (11.5 kcal/mol) thereby constitutes one of the lowest phosphorus inversion barriers on record.<sup>40</sup>

The phosphido substituents in symmetrically-substituted secondary complexes  $(\eta^5-C_5H_5)Re(NO)(PPh_3)(\dot{P}R_2)$  also readily exchange.<sup>4</sup> As diagrammed earlier, this process requires both phosphorus inversion and  $Re-\dot{P}R_2$  bond rotation. However, the  $\Delta G^\ddagger_{T(c)}$  are comparable to those in Table II ( $R$  = ethyl, 14.7–14.9 kcal/mol; *p*-tol, 13.0–13.3 kcal/mol; *tert*-butyl, 12.6 kcal/mol). In general, bulkier substituents lower phosphorus inversion barriers.<sup>40a</sup> However, meaningful trends in this limited sampling of compounds are difficult to identify. In other relevant work, Wild has found a  $\Delta G^\ddagger_{T(c)}$  of 14 kcal/mol for the interconversion of diastereomers of a chiral iron phenylphosphido complex  $(\eta^5-C_5H_5)Fe(PArAr'Me)_2(\dot{P}HPh)$  (9).<sup>3a</sup>

The highly diastereoselective methylation of 4c to  $(RS,SR)-5^+TfO^-$  has analogy in earlier work. For example, the carbanion  $Li^+[(\eta^5-C_5H_5)Re(NO)(PPh_3)(\dot{C}HCN)]^-$  and the ylide  $(\eta^5-C_5H_5)Re(NO)(PPh_3)(CH=P(p-tol)_3)$  both react with alkylating agents to give  $C_\alpha$  derivatives  $[(\eta^5-$



9

$C_5H_5)Re(NO)(PPh_3)(CHRX)]^{n+}$  in >98% de—but with opposite carbon configurations.<sup>41</sup> The stereochemistry of methylation of 4c is identical with that of the ylide.<sup>42</sup> Regardless, the rhenium fragment  $[(\eta^5-C_5H_5)Re(NO)-(PPh_3)]^+$  exerts an impressive degree of stereocontrol in the alkylation of a variety of types of adjacent nucleophilic centers.

In important related work, Wild has found that chiral iron phosphido complexes of the type 9 undergo similarly diastereoselective methylations.<sup>3</sup> He observes that the product diastereomer ratios match those of the precursor phosphido complexes, consistent with our results in Scheme V. Related auxiliary-based strategies for the diastereoselective synthesis of phosphine ligands have been described by Mathey.<sup>43</sup> When such chemistry is effected with optically active precursors, subsequent displacement reactions allow the generation of free optically active phosphines.

**5. Summary.** This study has established the ready availability of chiral primary phosphine and phosphido complexes  $2^+X^-$  and 4 in both racemic and optically active form, and systematized their intricate and unusual structural properties. Preliminary reactivity data have established the capability for highly stereoselective transformations. Although this concludes our present plans for exploratory synthetic and structural work in this area, the utility of these and related compounds as architectural units in reagents and catalysts for asymmetric transformations will receive future attention.

## Experimental Section

**General Data.** General procedures and instrumentation utilized were identical with those given in the previous paper,<sup>4b</sup> with the following additions. ORD/CD spectra were recorded on a JASCO J-20C spectrophotometer. Conductance measurements<sup>44</sup> were carried out on a Radiometer/Copenhagen CDM-3 conductivity meter with a platinum electrode, for which a cell constant of 0.115 was calculated from measurements with a 0.0200 M KCl solution (triply distilled  $H_2O$ ).

Reagents and solvents were obtained as described previously,<sup>4b</sup> with the following additions:  $HCl(g)$  (Matheson),  $TfOH$ , and  $LiAlH_4$  (Aldrich), used as received; DOTf, prepared by mixing  $Tf_2O$  (Alfa, distilled from  $P_2O_5$ ) and 1.0 equiv of  $D_2O$  in an ampule (4–5 days, until homogeneous), followed by distillation and  $^1H$  NMR assay,<sup>4b</sup>  $MeOTf$  (Aldrich) and  $PPhH_2$  (Pressure), distilled;

(41) Crocco, G. L.; Lee, K. E.; Gladysz, J. A. *Organometallics* 1990, 9, 2819.

(42) Stabilities of diastereomers of compounds of the type  $[(\eta^5-C_5H_5)Re(NO)(PPh_3)(CLMS)]^{n+}$ , where L/M/S are large, medium, and small-sized groups, have been extensively studied and analyzed.<sup>41</sup> Although a direct determination is not possible from our data,  $(RS,SR)-5^+TfO^-$  is certain to be more stable than  $(RR,SS)-5^+TfO^-$ . Thus, the methylation of 4c also gives the more stable of two possible diastereomers.

(43) de Vaumas, R.; Marinetti, A.; Ricard, L.; Mathey, F. *J. Am. Chem. Soc.* 1992, 114, 261.

(44) Angelici, R. J. *Synthesis and Technique in Inorganic Chemistry*, 2nd ed.; Saunders: Philadelphia, 1977; p 17.

(45) Bakos, H. J.; Ranson, R. J.; Roberts, R. M. G.; Sadri, A. R. *Tetrahedron* 1982, 38, 623.

(39) (a) For data with substituted cyclohexanes, see: Eliel, E. L.; Manoharan, M. *J. Org. Chem.* 1981, 46, 1959. (b) For data with  $[(\eta^5-C_5H_5)Re(NO)(PPh_3)(L)]^+X^-$  complexes, see: Peng, T.-S.; Arif, A. M.; Gladysz, J. A. *Helv. Chim. Acta* 1992, 75, 442. (c) Note that the  $^3J_{HP}$  values of  $(RR,SS)-4a$  and  $(RS,SR)-4a$  (ca. 10 and <2 Hz)<sup>39</sup> indicate distinctly different  $Ph_3P-Re-\dot{P}-H$  torsion angles, as would be expected from our proposal of slight counterclockwise  $Re-\dot{P}RH$  distortions in idealized structures II and III.

(40) (a) Rauk, A.; Allen, R. C.; Mislow, K. *Angew. Chem., Int. Ed. Engl.* 1970, 9, 400. (b) Schmidbauer, H.; Schier, A.; Lauteschläger, S.; Riede, J.; Müller, G. *Organometallics* 1984, 3, 1906. (c) Arduengo, A. J., III; Dixon, D. A.; Roe, D. C. *J. Am. Chem. Soc.* 1986, 108, 6821.

$P(t\text{-Bu})_2$ , prepared from  $P(t\text{-Bu})Cl_2$  (Strem),<sup>46</sup>  $O=P(OMe)_2Me$  (Strem), distilled from  $P_2O_5$ .

$[(\eta^5\text{-C}_5\text{H}_5)\text{Re}(\text{NO})(\text{PPh}_3)(\text{PPh}_2\text{H})]^+\text{TsO}^-$  ( $2a^+\text{TsO}^-$ ). A Schlenk flask was charged with  $(\eta^5\text{-C}_5\text{H}_5)\text{Re}(\text{NO})(\text{PPh}_3)(\text{OTf})$  (1;<sup>11</sup> 2.50 g, 3.50 mmol),  $\text{CH}_2\text{Cl}_2$  (50 mL), and a stir bar. Then  $\text{PPh}_2\text{H}$  (0.77 mL, 0.77 g, 7.00 mmol) was added with stirring. After 48 h, the solution was concentrated to ca. 25 mL. Ether was added, and the resulting yellow powder was collected by filtration, washed with ether, and air-dried to give  $2a^+\text{TsO}^-$  (2.72 g, 3.30 mmol, 94%). A sample was dissolved in  $\text{CH}_2\text{Cl}_2$ , and ether was slowly added by vapor diffusion. Yellow crystals formed, which were collected by filtration and dried under oil pump vacuum to give  $2a^+\text{TsO}^-$ , mp 208 °C dec. Anal. Calcd for  $\text{C}_{36}\text{H}_{24}\text{NO}_4\text{P}_2\text{ReS}$ : C, 52.42; H, 4.15; P, 7.51. Found: C, 52.17; H, 4.40; P, 7.31.

$[(\eta^5\text{-C}_5\text{H}_5)\text{Re}(\text{NO})(\text{PPh}_3)(\text{PMe}_2\text{H})]^+\text{TfO}^-$  ( $2b^+\text{TfO}^-$ ). **Caution:** The  $\text{PMe}_2\text{H}$  generated in this procedure<sup>47</sup> is volatile (bp  $-17$  °C), malodorous, and toxic. A well-ventilated fume hood is essential.

A 50-mL three-neck flask was fitted with two gas inlets with stopcocks and a septum-capped addition funnel. The flask was charged with  $\text{LiAlH}_4$  (0.80 g, 21 mmol), THF (15 mL), and a stir bar. The funnel was charged with  $O=P(OMe)_2Me$  (1.50 mL, 1.74 g, 14.0 mmol) and THF (2 mL). One gas inlet was attached to a vacuum manifold and the other to a vacuum adapter fitted to a Schlenk tube charged with  $(\eta^5\text{-C}_5\text{H}_5)\text{Re}(\text{NO})(\text{PPh}_3)(\text{OTf})$  (3;<sup>11</sup> 0.45 g, 0.65 mmol), toluene (20 mL), and a stir bar. The vacuum adapter on the Schlenk tube was fitted with a gas inlet with a stopcock that was attached via a glass "T" to an oil bubbler. The Schlenk tube stopcock was attached to the vacuum manifold.

The stopcocks connecting the Schlenk tube to the bubbler and three-neck flask were closed and the solution of 3 was freeze-pump-thaw degassed (3 $\times$ ). The solution was refrozen and left immersed in liquid  $\text{N}_2$  while  $\text{N}_2$  gas was carefully admitted from the three-neck flask. A gentle flow of  $\text{N}_2$  was begun from the three-neck flask through the Schlenk tube and bubbler. The  $\text{LiAlH}_4$  slurry was cooled to 0 °C and stirred. The  $O=P(OMe)_2Me$  solution was then carefully added at a rate conducive to the slow evolution of gaseous  $\text{PMe}_2\text{H}$  (warning: excessively rapid addition can give an uncontrollable evolution of  $\text{PMe}_2\text{H}$ ).<sup>48</sup>

Upon completion of the addition, the cold bath was removed from the three-neck flask. After 0.5 h, the vacuum adapter on the Schlenk tube was replaced with a securely fastened glass stopper. The tube was evacuated to prevent any pressure buildup, and the sample was thawed by immersion in a  $-80$  °C bath. The red solution was slowly warmed to room temperature with stirring. Within 15 min, a yellow solid precipitated. After 2 h, the tube was cooled to  $-80$  °C and  $\text{N}_2$  was carefully admitted. The stopper was removed and, under a  $\text{N}_2$  flow, the tube was warmed to room temperature to purge excess  $\text{PMe}_2\text{H}$ . The resulting pale yellow powder was collected by filtration, washed well with benzene, and dried under oil pump vacuum (1 h) to give  $2b^+\text{TfO}^-$  (0.46 g, 0.62 mmol, 96%) that was pure by  $^1\text{H}$  and  $^{31}\text{P}\{^1\text{H}\}$  NMR. The powder was dissolved in a minimum of THF and ether was added by vapor diffusion. Fine yellow needles formed which were collected by filtration and dried under oil pump vacuum (56 °C, 36 h) to give  $2b^+\text{TfO}^-$  (0.37 g, 0.49 mmol, 86%), mp 181–182 °C. Anal. Calcd for  $\text{C}_{25}\text{H}_{25}\text{F}_3\text{NO}_4\text{P}_2\text{ReS}$ : C, 40.54; H, 3.40; P, 8.36. Found: C, 41.08; H, 3.57; P, 7.89.

$[(\eta^5\text{-C}_5\text{H}_5)\text{Re}(\text{NO})(\text{PPh}_3)(\text{P}(t\text{-Bu})\text{H}_2)]^+\text{TfO}^-$  ( $2c^+\text{TfO}^-$ ). **A.** A Schlenk tube was charged with 3 (1.85 g, 2.67 mmol), benzene (50 mL), and a stir bar. Then  $\text{P}(t\text{-Bu})_2$  (0.490 mL, 0.360 g, 4.00 mmol) was added with stirring. After 3 h, hexane (10 mL) was added. The resulting yellow powder was collected by filtration, washed with hexane, and dissolved in a minimum of THF. Ether was slowly added by vapor diffusion. Yellow needles formed, which were collected by filtration and dried under oil pump vacuum (56 °C) to give  $2c^+\text{TfO}^-$  (1.86 g, 2.38 mmol, 89%), mp 211–213 °C dec. Anal. Calcd for  $\text{C}_{28}\text{H}_{31}\text{F}_3\text{NO}_4\text{P}_2\text{SRe}$ : C, 42.97;

H, 3.99. Found: C, 43.14; H, 4.18.

**B.** A Schlenk tube was charged with 4c (0.021 g, 0.033 mmol), benzene (5 mL), and a stir bar. Then HOTf (0.003 mL, 0.034 mmol) was added with stirring. After 5 min, hexane (10 mL) was added. The resulting pale yellow powder was collected by filtration, washed with hexane, and dried under oil pump vacuum to give  $2c^+\text{TfO}^-$  (0.016 g, 0.020 mmol, 62%).

$(\eta^5\text{-C}_5\text{H}_5)\text{Re}(\text{NO})(\text{PPh}_3)(\text{PPhH})$  (4a). A Schlenk flask was charged with  $2a^+\text{TsO}^-$  (3.80 g, 4.61 mmol), THF (210 mL), and a stir bar. Then  $t\text{-BuO}^-\text{K}^+$  (0.568 g, 5.07 mmol) was added with stirring. After 6 h, the mixture was filtered. The filtrate was concentrated to ca. 10 mL, and ether was added. The resulting precipitate was collected by filtration, washed with ether, and dried under oil pump vacuum. A small second crop was analogously isolated following further concentration of the filtrate. The crops were combined to give 4a (2.96 g, 4.53 mmol, 98%) as an air-sensitive orange-yellow powder. A sample was dissolved in THF, and hexane was added. Orange crystals formed, which were collected by filtration and dried under oil pump vacuum to give 4a, mp 182–184 °C dec. Anal. Calcd for  $\text{C}_{26}\text{H}_{26}\text{NOP}_2\text{Re}$ : C, 53.37; H, 4.02. Found: C, 53.10; H, 4.00. MS ( $m/e$ ,  $^{187}\text{Re}$ , 15 eV): 653 ( $M^+$ , 3%), 467 ( $M^+ - \text{PPh}_2\text{H}$ , 5%), 262 ( $\text{Ph}_3\text{P}^+$ , 100%), 183 ( $\text{Ph}_2\text{P}^+$ , 72%), 108 ( $\text{PhP}^+$ , 40%). UV (nm ( $\epsilon$ ), THF): 260 pk (12000), 273 sh (11000), 288 sh (10000), 315 sh (8400), 343 sh (6300).

$(\eta^5\text{-C}_5\text{H}_5)\text{Re}(\text{NO})(\text{PPh}_3)(\text{PMeH})$  (4b). A flask was charged with  $2b^+\text{TfO}^-$  (0.20 g, 0.27 mmol), THF (20 mL), and a stir bar. Then  $t\text{-BuO}^-\text{K}^+$  (0.033 g, 0.30 mmol) was added with stirring. After 5 min, solvent was removed under oil pump vacuum. The orange residue was extracted with benzene, and the extract was filtered through  $\text{C}_6\text{elite}$ . The filtrate was concentrated, and hexane was slowly added by vapor diffusion. Orange needles formed, which were collected by filtration and dried under oil pump vacuum (56 °C, 36 h) to give 4b ( $\text{C}_8\text{H}_8$ )<sub>0.25</sub> (0.10 g, 0.17 mmol, 63%), mp 191–193 °C. Anal. Calcd for  $\text{C}_{24}\text{H}_{24}\text{NOP}_2\text{Re}(\text{C}_8\text{H}_8)_{0.25}$ : C, 50.20; H, 4.21; P, 10.15. Found: C, 49.81; H, 4.27; P, 9.87. The presence of the solvate was verified by  $^1\text{H}$  NMR ( $\delta$ , THF- $d_6$ ): 7.20. UV (nm ( $\epsilon$ ),  $3.1 \times 10^{-4}$  M in THF): 243 sh (6006);  $\epsilon = 552$  at 400 nm.

$(\eta^5\text{-C}_5\text{H}_5)\text{Re}(\text{NO})(\text{PPh}_3)(\text{P}(t\text{-Bu})\text{H})$  (4c). Complex  $2c^+\text{TfO}^-$  (1.00 g, 1.28 mmol), THF (25 mL), and  $t\text{-BuO}^-\text{K}^+$  (0.16 g, 1.4 mmol) were combined in a procedure analogous to that given for 4b. An identical workup gave orange needles of 4c (0.63 g, 1.0 mmol, 78%), mp 199–202 °C. Anal. Calcd for  $\text{C}_{27}\text{H}_{30}\text{NOP}_2\text{Re}$ : C, 51.26; H, 4.78; P, 9.79. Found: C, 51.46; H, 4.99; P, 9.78. UV (nm ( $\epsilon$ ),  $1.9 \times 10^{-4}$  M in THF): 266 sh (8560), 317 sh (3210);  $\epsilon = 749$  at 400 nm.

**Optically Active Complexes.** **A.** Complex  $(-)(S)\text{-}2c^+\text{TfO}^-$  was synthesized from  $(-)(S)\text{-}3^{11}$  on a 0.72-mmol scale by a procedure analogous to that given for the racemate. Workup gave  $(-)(S)\text{-}2c^+\text{TfO}^-$  as a yellow powder (0.50 g, 0.60 mmol, 88%),  $[\alpha]_D^{25} -141^\circ$  ( $c = 1.0$  mg/mL,  $\text{CHCl}_3$ ), which was pure by  $^1\text{H}$  and  $^{31}\text{P}\{^1\text{H}\}$  NMR (data similar to those of racemate). ORD (nm,  $c = 2.0$  mg/mL,  $\text{CHCl}_3$ ;  $l = 1$  cm): 0 at 700, 399; minimum at 432 ( $[\alpha]^{22} -0.0204^\circ$ ); maximum at 356 ( $[\alpha]^{22} 0.0315^\circ$ ). CD (nm,  $c = 1.0$  mg/mL,  $\text{CHCl}_3$ ;  $l = 1$  cm): 0 at 700, 334, 316, 285; minima at 394 ( $[\theta]^{22} -0.182^\circ$ ), 298 (local); maximum at 326 ( $[\theta]^{22} 0.012^\circ$ ).

**B.** Complex  $(-)(S)\text{-}4c$  was synthesized from  $(-)(S)\text{-}2c^+\text{TfO}^-$  on a 0.32-mmol scale by a procedure analogous to that given for the racemate. Workup gave  $(-)(S)\text{-}4c$  as an orange foam (0.015 g, 0.23 mmol, 72%),  $[\alpha]_D^{20} -125^\circ$  ( $c = 1.0$  mg/mL, THF), which was pure by  $^1\text{H}$  and  $^{31}\text{P}\{^1\text{H}\}$  NMR (data similar to those of racemate). ORD (nm,  $c = 1.0$  mg/mL, THF;  $l = 1$  cm): 0 at 650 and 423; minima at 464 ( $[\alpha]^{22} -0.0052^\circ$ ), 349 (local); maximum at 383 ( $[\alpha]^{22} 0.0095^\circ$ ). CD (nm,  $c = 1.0$  mg/mL, THF;  $l = 1$  cm): 0 at 650, 368, 357, 327; minima at 414 ( $[\theta]^{22} -0.107^\circ$ ), 337 (local); maximum at 363 ( $[\theta]^{22} 0.0058^\circ$ ).

$[(\eta^5\text{-C}_5\text{H}_5)\text{Re}(\text{NO})(\text{PPh}_3)(\text{P}(t\text{-Bu})\text{MeH})]^+\text{TfO}^-$  ( $5^+\text{TfO}^-$ ). **A.** A Schlenk flask was charged with 4c (0.40 g, 0.63 mmol), benzene (20 mL), and a stir bar. Then  $\text{MeOTf}$  (0.11 mL, 0.95 mmol) was added. After 5 min, hexane (10 mL) was added to the cloudy yellow mixture. The resulting yellow precipitate was collected by filtration and dried under oil pump vacuum (56 °C) to give  $(RS,SR)\text{-}5^+\text{TfO}^-$  (0.48 g, 0.60 mmol, 95%) that was pure by  $^1\text{H}$  and  $^{31}\text{P}\{^1\text{H}\}$  NMR. The sample was dissolved in THF, and ether was slowly added by vapor diffusion. Yellow needles formed, which were collected by filtration and dried under oil pump

(46) Becker, V. G.; Mundt, O.; Rössler, M.; Schneider, E. Z. *Anorg. Allg. Chem.* 1978, 443, 42.

(47) De, R. L.; Vahrenkamp, H. Z. *Naturforsch.* 1985, 40b, 1250.

(48) In a separate experiment, the  $\text{PMe}_2\text{H}$  generated was trapped in cold  $\text{CDCl}_3$  and shown to be spectroscopically pure.  $^{31}\text{P}$  NMR (ppm, 32.3 MHz):  $-161.4$  (br t,  $J_{\text{PH}} = 193$  Hz).  $^1\text{H}$  NMR ( $\delta$ ): 2.52 (br d,  $J_{\text{HP}} = 190.6$  Hz, 2H), 0.86 (br s, 3H).

vacuum to give  $(RS,SR)\text{-}5^+\text{TfO}^-$  (0.43 g, 0.54 mmol, 85%), mp 218–220 °C dec. Anal. Calcd for  $\text{C}_{29}\text{H}_{33}\text{F}_3\text{NO}_4\text{P}_2\text{SRe}$ : C, 43.72; H, 4.17; P, 7.77. Found: C, 43.62; H, 4.26; P, 8.20.

B. A Schlenk flask was charged with **6** (0.25 g, 0.39 mmol), benzene (15 mL), and a stir bar. The HOTf (0.038 mL, 0.43 mmol) was added with stirring. After 5 min, hexane (5 mL) was added. The resulting yellow powder was collected by filtration and dried under oil pump vacuum to give  $5^+\text{TfO}^-$  (0.29 g, 0.36 mmol, 93%), which  $^1\text{H}$  and  $^{31}\text{P}\{^1\text{H}\}$  NMR showed to be an  $(80 \pm 2):(20 \pm 2)$  mixture of  $RS,SR/RR,SS$  diastereomers.

$(\eta^5\text{-C}_5\text{H}_5)\text{Re}(\text{NO})(\text{PPh}_3)(\text{P}(t\text{-Bu})\text{Me})$  (**6**). A Schlenk flask was charged with  $(RS,SR)\text{-}5^+\text{TfO}^-$  (1.01 g, 1.28 mmol), THF (30 mL), and a stir bar. Then  $t\text{-BuO}^-\text{K}^+$  (0.16 g, 1.4 mmol) was added with stirring. After 5 min, solvent was removed under oil pump vacuum. The red residue was extracted with toluene, and the extract was filtered through Celite. The filtrate was concentrated to 6–8 mL and then kept at 80 °C until all of the sample dissolved. The solution was slowly cooled to –20 °C. After 24 h, the resulting deep red prisms were collected by filtration and dried under oil pump vacuum (56 °C) to give **6** (0.67 g, 1.0 mmol, 81%), mp 192–194 °C dec. Anal. Calcd for  $\text{C}_{29}\text{H}_{32}\text{NOP}_2\text{Re}$ : C, 52.00; H, 4.99; P, 9.58. Found: C, 51.86; H, 5.04; P, 9.27. UV (m  $\epsilon$ ),  $3.2 \times 10^{-4}$  M in THF): 303 sh (5140);  $\epsilon = 1050$  at 400 nm.

$[(\eta^5\text{-C}_5\text{H}_5)\text{Re}(\text{NO})(\text{PPh}_3)(\text{P}(t\text{-Bu})\text{H}_2)]^+\text{Cl}^-$  ( $2\text{c}^+\text{Cl}^-$ ). A three-neck flask was charged with **4c** (0.20 g, 0.32 mmol), benzene (15 mL), and a stir bar and fitted with a rubber septum and two gas inlets with stopcocks. A needle was inserted through the septum, and HCl gas was passed over the stirred solution, which immediately turned from orange to yellow. After 5 min, the flask was purged with  $\text{N}_2$ , and hexane (20 mL) was added. An oily, yellow residue deposited on the flask walls. The colorless supernatant was decanted, and the residue was dried under oil pump vacuum (3 h) to give  $2\text{c}^+\text{Cl}^-$  as a spectroscopically pure yellow foam (0.19 g, 0.28 mmol, 89%).

**Crystal Structures.** A. Hexane was carefully layered onto a  $\text{CH}_2\text{Cl}_2$  solution of  $2\text{c}^+\text{Cl}^-$ . Yellow/green irregular prisms formed, which were collected by filtration and dried under a  $\text{N}_2$  flow to give  $2\text{c}^+\text{Cl}^- \cdot 0.5\text{CH}_2\text{Cl}_2$ . Anal. Calcd for  $\text{C}_{27}\text{H}_{31}\text{ClINOP}_2\text{Re} \cdot 0.5\text{CH}_2\text{Cl}_2$ : C, 46.42; H, 4.53; Cl, 9.96. Found: C, 45.98; H, 4.54; Cl, 10.06. Data were collected on a Syntex P1 diffractometer as described in Table III. Cell constants were obtained from 15 reflections in the range  $20^\circ < 2\theta < 24^\circ$ . The space group was determined from systematic absences ( $0kl$ ,  $k = 2n$ ;  $h0l$ ,  $l = 2n$ ;  $hkl$ ,  $h = 2n$ ) and subsequent least-squares refinement. Standard reflections showed no decay during data collection. Lorentz, polarization, and empirical absorption ( $\psi$  scans) corrections were applied to the data. The structure was solved by standard heavy-atom techniques with the SDP-VAX package.<sup>49</sup> All non-hydrogen atoms, except those in the solvate,

were refined with anisotropic thermal parameters. The PH hydrogen atoms were located, and other hydrogen atom positions were calculated. These were added to the structure factor calculations but not refined. Scattering factors, and  $\Delta f'$  and  $\Delta f''$  values, were taken from the literature.<sup>50</sup> B. An identical crystallization gave a yellow elongated prism of  $(RS,SR)\text{-}5^+\text{TfO}^-$ , and X-ray data were similarly collected. The cell constants and space group were analogously determined (36 reflections,  $10^\circ < 2\theta < 20^\circ$ ; systematic absences  $h0l$ ,  $l = 2n$ ;  $0k0$ ,  $k = 2n$ ). The structure was solved in a comparable manner, except that the PH hydrogen was refined.

**NMR Experiments.** A. General procedures for dynamic NMR experiments<sup>19</sup> have been described earlier.<sup>4b</sup> Near coalescence temperatures, spectra were acquired at 1–2-deg intervals after a 15-min thermal equilibration period. Additional details are given elsewhere.<sup>8</sup>

B. Homonuclear  $^1\text{H}$  NOE difference spectra<sup>18</sup> were acquired at 21.6 °C on sealed samples of  $2\text{c}^+\text{TfO}^-$  and  $(RS,SR)\text{-}5^+\text{TfO}^-$  (0.10 M in  $\text{CDCl}_3$ ) that had been freeze–pump–thaw degassed (3 $\times$ ). Each experiment was performed as an array consisting of two spectra: the first was obtained with 65–91% irradiation of the cyclopentadienyl resonance and the second (off-resonance) was obtained with the decoupler frequency set  $>2$  ppm from all resonances. Spectra were obtained in interleaved blocks of 32 transients with four steady-state transients per block for a total of 2048 transients (acquisition time 2.99 s; pulse delay 6 s). The  $T_1$  values of the PH protons of  $2\text{c}^+\text{TfO}^-$  were determined in a separate experiment to be 0.50 and 0.53 s (less than 10% of pulse delay). The off-resonance spectrum was subtracted from the cyclopentadienyl irradiated spectrum to give the difference NOE data.

**Acknowledgment.** We thank the NSF for support of this research.

**Supplementary Material Available:** Tables of anisotropic thermal parameters for  $2\text{c}^+\text{Cl}^- \cdot 0.5\text{CH}_2\text{Cl}_2$  and  $(RS,SR)\text{-}5^+\text{TfO}^-$  (2 pages). Ordering information is given on any current masthead page.

OM920089K

(49) Frenz, B. A. The Enraf-Nonius CAD 4 SDP—A Real-time System for Concurrent X-ray Data Collection and Crystal Structure Determination. In *Computing and Crystallography*; Schenk, H., Olthof-Hazelkamp, R., van Koningsveld, H., Bassi, G. C., Eds.; Delft University Press: Delft, Holland, 1978; pp 64–71.

(50) Cromer, D. T.; Waber, J. T. In *International Tables for X-ray Crystallography*; Ibers, J. A.; Hamilton, W. C., Eds.; Kynock: Birmingham, England, 1974; Vol IV, tables 2.2B and 2.3.1.